

The effects of climate change and extreme wildfire events on runoff erosion over a mountain watershed



Gregory K. Gould^a, Mingliang Liu^a, Michael E. Barber^{a,1}, Keith A. Cherkauer^b, Peter R. Robichaud^c, Jennifer C. Adam^{a,*}

^a Department of Civil & Environmental Engineering, Washington State University, Pullman, WA 99163, USA

^b Department of Agricultural & Biological Engineering, Purdue University, West Lafayette, IN 47907, USA

^c Rocky Mountain Research Station, USDA Forest Service, Moscow, ID 83843, USA

ARTICLE INFO

Article history:

Received 25 September 2015

Received in revised form 11 February 2016

Accepted 15 February 2016

Available online 23 February 2016

This manuscript was handled by Tim R.

McVicar, Editor-in-Chief, with the assistance of Patrick Norman Lane, Associate Editor

Keywords:

Wildfire
Erosion
Climate change
WEPP model
Hydrology

SUMMARY

Increases in wildfire occurrence and severity under an altered climate can substantially impact terrestrial ecosystems through enhancing runoff erosion. Improved prediction tools that provide high resolution spatial information are necessary for location-specific soil conservation and watershed management. However, quantifying the magnitude of soil erosion and its interactions with climate, hydrological processes, and fire occurrences across a large region (>10,000 km²) is challenging because of the large computational requirements needed to capture the fine-scale complexities of the land surface that govern erosion. We apply the physically-based coupled Variable Capacity Infiltration–Water Erosion Prediction Project (VIC–WEPP) model to study how wildfire occurrences can enhance soil erosion in a future climate over a representative watershed in the northern Rocky Mountains – the Salmon River Basin (SRB) in central Idaho. While the VIC model simulates hydrologic processes at larger scales, the WEPP model simulates erosion at the hillslope scale by sampling representative hillslopes.

VIC–WEPP model results indicate that SRB streamflow will have an earlier shift in peak flow by one to two months under future climate scenarios in response to a declining snowpack under warming temperatures. The magnitude of peak flow increases with each higher severity fire scenario; and under the highest fire severity, the peak flow is shifted even earlier, exacerbating the effects of climate change. Similarly, sediment yield also increases with higher fire severities for both historical and future climates. Sediment yield is more sensitive to fire occurrence than to climate change by one to two orders of magnitude, which is not unexpected given that our fire scenarios were applied basin wide as worst case scenarios. In reality, fires only occur over portions of the basin in any given year and subsequent years' vegetation regrowth reduces erosion. However, the effects of climate change on sediment yield result in greater spatial heterogeneities, primarily because of the spatial differences in precipitation projections, while fire conditions were uniformly applied. The combined effects of climate change and a possible continuation of increasing fire frequency and severity will compound excess sediment issues that already exist in this region of the intermountain West.

© 2016 Elsevier B.V. All rights reserved.

1. Introduction

Climate change is expected to increase the frequency, duration, and intensity of extreme weather events and associated droughts, wildfires, and rainfall events (Karl et al., 2008), all of which can change streamflow volumes and sediment concentrations. Policies around fire suppression and exclusion contributed to altered wild-

fire activity in the western U.S. (Stephens and Ruth, 2005). The burned area by wildfires in central Idaho increased by 14 times between the periods of 2001–2010 and 1971–1980 (U.S. Army Corps of Engineers, 2012). While periodic wildfire is a necessary process for maintaining overall forest health (Agee, 1993), there are a number of negative impacts that can result to the environment, such as through decreasing infiltration rates and increasing overland flow (Moody and Martin, 2009; Robichaud et al., 2010), increasing soil erosion (Benavides-Solorio and MacDonald, 2005, 2001; Connaughton, 1935; DeBano et al., 2005; Doerr et al., 2006; Helvey, 1980; Holden et al., 2012; Johansen et al., 2001;

* Corresponding author.

E-mail address: jcadam@wsu.edu (J.C. Adam).

¹ Present address: Department of Civil & Environmental Engineering, The University of Utah, Salt Lake City, UT 84112, USA.

Larsen et al., 2009; Moody and Martin, 2009) and degrading water quality (Reneau et al., 2007).

Erosion and excess sediment can affect ecosystems and waterways by adversely impacting aquatic life, navigation, reservoir sedimentation and flood storage, drinking water supply, and aesthetics (Espinosa et al., 1997; Owens et al., 2005; Robertson et al., 2007; Wood and Armitage, 1997). In the Pacific Northwest (PNW), Teasdale and Barber (2008) and other researchers found that forest wildfires likely provide a large percent of the coarser sands that settle in navigation channels and in reservoirs (Boll et al., 2011; Elliot, 2013). Goode et al. (2012) predicted that sediment yields could potentially increase by ten-fold from observed long-term rates in central Idaho because of increased wildfire burn severity and extent. Climate change may also impact sediment yield from burned landscapes. The PNW is facing reduced summer soil moisture and streamflow due to a warming-induced declining snowpack in this winter-dominant precipitation region (Leung et al., 2004; Miles et al., 2000; Mote et al., 2005; US Global Change Research Program, 2012). This shift toward mixed (rain/snow) or rain-dominant precipitation can have implications for increased sediment generation during the winter and spring; while changes in summer rainfall events will impact summer erosion rates. Given the complexity of factors that can impact post-fire sediment generation, there is still much unknown as to how future climate and burn severity/extent interactively affect the magnitude of post-fire soil erosion in different locations in the intermountain western U.S.

Numerous empirical and mechanistic soil erosion models have been developed since the 1950s. A brief review on the model developments and major research activities related to this research question is listed in Table 1. The universal soil loss equation (USLE) provided a powerful, empirical tool to estimate erosion (Renard et al., 1991; Wischmeier and Smith, 1978). USLE estimates average annual soil loss through a series of factors that relate to climate, soil erosivity, topography, land use, and land management (Wischmeier and Smith, 1978). As it was applied broadly, many updated versions, including the revised universal soil loss equation (RUSLE; (Renard et al., 1991)), the modified USLE (MUSLE; (Williams and Berndt, 1977)), and RUSLE2 (Foster et al., 2000; Lown et al., 2000) have been produced during the last several decades (Table 1). However, these empirical tools normally are location-specific, and intensive model calibrations are required for applications over different places (Lafren et al., 1991). The Water Erosion Prediction Project (WEPP) model is a continuous process-based model developed by the U.S. Department of Agriculture – Agricultural Research Service (USDA–ARS), which includes detachment, transport, and deposition processes (Flanagan and Nearing, 1995) (Table 1). Because of its mechanistic nature, the WEPP model requires much less calibration than the more empirical USLE and RUSLE methods (Mao et al., 2010). To allow users to estimate erosion after a disturbance, the Disturbed-WEPP web interface was developed which contains several default parameters and vegetation treatments (Elliot and Hall, 2010). As the processes governing runoff erosion are fine-scale in nature, the WEPP model (as well as other watershed-scale erosion models, e.g. (Arnold et al., 1998; Leonard et al., 1987; Williams et al., 1985)) was originally developed at the hillslope scale. This makes it difficult to evaluate the overall effectiveness of land use policy and the implementation of conservation programs, which normally occur over watershed and regional scales (Mao et al., 2010) (Table 1). Therefore, a framework to nest this relatively fine-scale model into a larger-scale framework is needed. Mao et al. (2010) linked hydrologic outputs from the Variable Infiltration Capacity (VIC) macro-scale hydrologic model (Liang et al., 1994) with the erosion module from WEPP (WEPP-Hillslope Erosion, WEPP-HE) (Flanagan et al., 2005) to estimate soil erosion over thousands of square kilometers.

However, this VIC–WEPP model implementation has no specific parameterizations on fire disturbances; these disturbances are a new addition in this study.

The overall goal of this study is to quantify the relative roles and combined impacts of climate change and extreme wildfires in contributing to runoff-induced sediment generation at larger scales across the PNW. To do this, we refined the VIC–WEPP model for post-fire conditions and applied the model over the Salmon River Basin (SRB), a relatively human unimpaired watershed in the U.S. intermountain West. We predict the influence of climate change and wildfire severity on streamflow regimes and sediment generation patterns.

2. Study domain

The SRB is located in the central of Idaho and lies between the Rocky Mountains on the east and the Columbia Plateau on the northwest and its elevation ranges from 304 to 3713 m (Fig. 1). It is one of the largest undeveloped watersheds in the U.S. (~36,000 km²) with 27% of the basin federally protected and nearly 90% owned by the Bureau of Land Management (BLM) and the U.S. Forest Service (USFS) (Tetra Tech EC, Inc., 2006).

The sediment contributions from the SRB play an important role with respect to flood control, irrigation, infrastructure, and navigation in the Lower Snake River (LSR) (U.S. Army Corps of Engineers, 2012). About 54% of the total sediment (65% of the total sand) entering the Lower Granite Reservoir was generated from the SRB during 2008–2011 (U.S. Army Corps of Engineers, 2012). As the primary source of sediment yield from the SRB comes from disturbed areas such as wildfire and roads (Goode et al., 2012), predicting post-fire soil erosion is critical for reservoir and environmental management. During the period of 2001–2010, wildfire affected approximately 7200 km² in the SRB as compared to 500 km² during 1971–1980 (U.S. Army Corps of Engineers, 2012).

Climate change is also projected to play an important role in the hydrologic processes that govern runoff-induced erosion. Other studies have involved application of the VIC model to understand the implications of climate change on SRB hydrology and have found that warming results in an earlier shift in the timing of the snowmelt peak (Sridhar et al., 2013; Tang and Lettenmaier, 2012) and that overall basin runoff may increase by a small amount under future climate scenarios (Sridhar et al., 2013).

3. Methods

3.1. Implementation of the coupled VIC–WEPP model

In this study, we refined and applied the VIC–WEPP modeling framework which was originally developed by Mao et al. (2010). The VIC model (v4.1.1) is a fully-distributed, physically-based macro-scale hydrologic model which solves the water and energy budgets at every time step (from 1 to 24 h) and for every grid cell (Liang et al., 1994). It is developed for large-scale applications (1/16th–2°), in which sub-grid variability in land cover, topography, and saturated extent is based on statistical relationships. The VIC model accounts for key moisture and energy fluxes between the land surface and the atmosphere and includes algorithms for shallow subsurface (frozen and unfrozen) moisture, snow, lake, and wetland dynamics (Andreadis et al., 2009; Bowling and Lettenmaier, 2010; Cherkauer and Lettenmaier, 1999). The VIC model has been applied over all continental land areas, and has been extensively used over the western U.S. (e.g., Hamlet and Lettenmaier, 1999; Maurer et al., 2002; Elsner et al., 2010; Hamlet et al., 2013; Liu et al., 2013) as well as the SRB

Table 1
Summary of relevant research on occurrences of wildfire and its effects on runoff and erosion over mountainous regions.

#	Country: Location/Land-cover	Reference (R) Data/Model (D/M) Location/ Land-cover (L/L)	Key results/limitations (or comments)
1	Global: global scale/all ecosystems	R: Chuvieco et al. (2014) D/M: ORCHIDEE/USLE	<ul style="list-style-type: none"> Generated a global fire vulnerability map. Two components are used for estimating soil erosion potential: potential soil degradation and adaptation to fire. The vulnerability levels to the soil erosion potential was carried out by cross-tabulation procedures (i.e. more descriptive and empirical than process-based) and used a coarse resolution DEM and climate data directly without any spatial disaggregation treatments; therefore, it has many uncertainties for local and regional applications.
2	Global: global	R: Moody et al. (2013) , Ebel and Moody (2013) and Moody and Martin (2014) D/M: literature review	<ul style="list-style-type: none"> Identified research priorities related to post-fire runoff and erosion response: to (1) understand the relations between soil properties and burn severity metrics; (2) characterize meso-scale rainfall appropriately; (3) develop new methods for determining sediment supply and modifying existing sediment transport algorithms; and (4) develop standard measurement methods for collecting uniform and comparable runoff and erosion data. Post-fire responses can be organized into domains with three quantifiable metrics for the fire, precipitation, and hydro-geomorphic regimes. The hyper-dry domain is important for understanding post-fire infiltration-runoff response. Effects of soil–water repellency should be incorporated into infiltration models. There is a lack of models to predict post-wildfire channel scour, bank erosion, and biological effects on sediment transport. Physically-based models are needed to investigate the effects of single variables on runoff and erosion.
3	Global: global	R: Nyman et al. (2013) D/M: literature review	<ul style="list-style-type: none"> Current post-fire response models are largely designed to predict catchment processes after a fire event; while new models are needed to predict larger-scale implications of climate change and fire management on longer-term catchment processes. Landscape-scale interactions between fires, catchment processes, and fire regimes should include: (1) first-order interactions between rain storms and fire events; (2) the coincidence of fire impacts and rain storms in spatial and temporal dimensions; and (3) linkages between long-term erosion rate and event frequencies.
4	USA: Colorado Front Range/pine forests	R: Benavides-Solorio and MacDonald (2001) D/M: Field OBS ^a /EXP ^b	<ul style="list-style-type: none"> Burn severity has only slight effects on runoff rate. Burn severity has a very large effect on sediment yield (and percent ground cover explained 81% of the variety in sediment yield). The plots are too short to generate rill erosion.
5	USA: Buffalo Creek & Spring Creek, Colorado/sparsely forested	R: Moody and Martin (2001a) D/M: Catchment OBS	<ul style="list-style-type: none"> The relaxation or recovery time in runoff and erosion responses are much less than the fire recurrence interval. Rill, interrill, and drainage erosion accounts for 6%, 14%, and 80% of the initial erosion in the observed wildfire occurrence year (i.e. 1996), respectively. Erosional and depositional features caused by wildfire may become legacies and become a new set of initial conditions for subsequent wildfire and flood sequences as the estimated residence time of eroded sediment is greater than 300 years.
6	USA: Three watersheds in South Dakota (Bear Gulch), Colorado (Spring Creek), and New Mexico (Rendija Canyon)/N.A.	R: Moody and Martin (2001b) and Moody et al. (2008) D/M: Catchments OBS	<ul style="list-style-type: none"> Post-fire changes in peak discharge (1.45 to 870-fold increase) are much larger than post-fire changes in annual runoff (0.5-fold decrease to a 4.5-fold increase) (conclusion from literature review). These three burned mountainous watersheds show that rainfall–runoff relations exist that relate the unit-area peak discharge to the maximum 30 min rainfall intensity (I_{30}) by a power law. Above the threshold ($I_{30} \sim 10 \text{ mm h}^{-1}$) the flood peaks increases more rapidly. The reason for the existence of the threshold could be the change in the infiltration rate by wildfire and/or the nature of hillslope friction. The threshold may change with time and perhaps approach the pre-fire condition.

Table 1 (continued)

#	Country: Location/Land-cover	Reference (R) Data/Model (D/M) Location/ Land-cover (L/L)	Key results/limitations (or comments)
7	USA: western United States/various ecosystem types	R: Moody and Martin (2009) D/M: literature review (data synthesis)	<ul style="list-style-type: none"> The erosion response did not vary significantly between the granitic terrain (Spring Creek) and volcanic terrains (Rendija Canyon). A dataset of post-fire sediment erosion, transport, and deposition measurements (135) was compiled from literature (1927–2007) for the western U.S. where measurements were made within 2-years after wildfire. Post-fire sediment yield from channels were greater than yields from hillslopes across the western U.S.; i.e. ~75% of the post-fire sediment yield comes from channels and 25% comes from hillslopes. Wildfire was an important geomorphic agent of landscape change when sufficient rainfall follows. <i>Quantitative information on burn severity, rainfall intensity, overland flow discharge, channel geometry, and channel discharge is limited for understanding the complex links between climate, rainfall, land cover, wildfire, and sediment yields.</i>
8	USA: Front Range Foothills in Colorado, near Boulder/Montane ecosystem	R: Ebel et al. (2012) D/M: Catchment OBS	<ul style="list-style-type: none"> Burned area has a large reduction in water infiltration into soils. Ash acts as an important hydrologic buffer by storing water readily after storm and releasing it slowly over a period of several days into the soil and by evaporation to the air. <i>Hydrologic models should include ash-controlled hydrologic processes and runoff generation mechanisms in estimating peakflow rate and total amounts of runoff in the few months after wildfire.</i>
9	USA: Lower Snake River Basin/Croplands	R: Boll et al. (2011) D/M: GIS-based RUSLE (i.e. RUSLE2) and WEPP	<ul style="list-style-type: none"> The highest erosion rates occur in high precipitation zones and with conventional tillage practices. <i>Not enough long-term data to evaluate and calibrate models.</i>
10	USA: Northwestern U.S.	R: Elliot (2013) and Elliot and Hall (2010) D/M: Overview/Disturbed WEPP	<ul style="list-style-type: none"> Wildfire is the natural disturbance that generates the greatest amount of sediment in the western U.S. <i>Prediction models, e.g. WEPP, ERMit, etc., are usable for hillslope and road segment processes, but improvements are made in incorporating road networks, flood routing, and spatial variability associated with wildfire burn severity and weather at watershed scales.</i>
11	USA: The central Idaho/coniferous forests	R: Goode et al. (2012) D/M: Synthesis of existing data	<ul style="list-style-type: none"> The extent and frequency of wildfires are expected to increase in the next several decades because warming may likely extend the fire season throughout the western U.S. <i>Cumulative effects of grazing on basin-scale sediment yield should to be addressed.</i>
12	USA: North central Washington/mixed conifer forests	R: Helvey (1980) D/M: Catchment OBS	<ul style="list-style-type: none"> Runoff increases after wildfire, particularly during subsequent years. Sediment production increased dramatically after the fire due to increased flow rates, overland flow, and mass soil movement.
13	USA: Pacific Northwest USA/forests	R: Holden et al. (2012) D/M: Satellite-derived burnt area and severity	<ul style="list-style-type: none"> Annual area burnt and area burn severity are strongly and positively correlated. The annual area burnt and severity are significantly correlated with metrics of total annual streamflow and streamflow timing. <i>Interacting effects of climate, topography, vegetation, and land use on wildfire extent and severity should be considered.</i>
14	USA: Near Los Alamos, New Mexico, USA/semiarid forest	R: Johansen et al. (2001) D/M: Field EXP	<ul style="list-style-type: none"> Post-fire sediment yields increase non-linearly as percent bare soil increases. There is a limited effect of water repellency on runoff from burned plots. Large increases in sediment yields follow severe fire in a pine forest, which is an order of magnitude greater than most other ecosystems. <i>The persistence of increases in post-fire sediment and water yields needs to be studied.</i>
15	USA: U.S./rangeland and cropland	R: Lafren et al. (1991) D/M: Field EXP/WEPP	<ul style="list-style-type: none"> Interrill and rill erodibility and critical hydraulic shear must be estimated when using WEPP; they are poorly correlated with USLE soil erodibility values. Rill and interrill erodibilities for rangelands are much lower than for cropland soils. <i>Extensive field data need to be collected when using WEPP.</i>

(continued on next page)

Table 1 (continued)

#	Country: Location/Land-cover	Reference (R) Data/Model (D/M) Location/ Land-cover (L/L)	Key results/limitations (or comments)
16	USA: Colorado Front Range/ponderosa pine and some Douglas pine	R: Larsen et al. (2009) D/M: Field OBS/EXP and laboratory-based study	<ul style="list-style-type: none"> Hillslopes with high severity burns results in stronger soil water repellency than unburned hillslopes only for the first summer, but sediment yields from these burnt areas are greatly elevated about background levels for several years. Removing the surface litter by raking has similar effects to that of rainfall on sediment yields over burned hillslopes. There is close relationship between surface cover percentage and post-fire sediment yield which is caused by soil sealing rather than soil water repellency or fire-induced changes in soil erodibility. <i>The most effective post-fire rehabilitation treatments will be increasing surface cover.</i>
17	USA: Minnesota/cropland, forest, and prairie grassland	R: Mao et al. (2010) D/M: Coupled VIC/WEPP-HE model	<ul style="list-style-type: none"> The coupling of the large-scale hydrology model (i.e. VIC) and the WEPP hillslope erosion model is able to predict soil erosion at large river basin scales. Discrepancies between coupled model results and the stand-alone WEPP model arise from differences in hydrologic processes and simplifications in vegetation and soil erodibility. <i>The model's performance in responding to disturbances such as wildfire should to evaluated.</i> <i>Sediment transport from each VIC grid cell into the stream needs to be addressed.</i>
18	USA: U.S.	R: Renard et al. (1991) D/M: USLE/RUSLE	<ul style="list-style-type: none"> An improved iso-erodent map for the western U.S.; new approaches for estimating K factor and its seasonality; a sub-factor method for computing soil loss ratios (i.e., a revised C factor); new P-factor considering the effect of terracing and contouring. USLE/RUSLE adequately captures the first-order effects of the major factors controlling sheet and rill erosions. <i>USLE/RUSLE estimates average annual soil loss due to sheet and rill erosion over the portion of landscape without deposition occurring.</i> <i>USLE/RUSLE is an empirically-based model and does not simulate hydrologic and erosion processes explicitly.</i>
19	USA: Cerro Grande burn area, New Mexico, U.S.	R: Reneau et al. (2007) D/M: Filed OBS	<ul style="list-style-type: none"> Over 90% of the ash was delivered to the reservoir by relatively moderate convective storms in the summer after the burn. Fine-grained sediment delivery rapidly declined after the wildfire, while delivery of coarse-grained sediment was prolonged. Impacts of ash and other fine grained sediment on reservoirs occurred soon after the fire, whereas the downstream impacts of coarse-grained sediment attenuated gradually by bedload sediment transport which correlated with snowmelt.
20	USA: Northern Rocky Mountain forest/coniferous forest	R: Robichaud (2000) D/M: Field EXP/OBS	<ul style="list-style-type: none"> High-severity burn sites produce greater runoff rates than low-severity sites especially during the initial stages of the first rainfall event. The hydrophobicity caused by prescribed fire can be washed away within one to two years. Cumulative distribution algorithms of hydraulic conductivity can be used with an erosion model as they account for inherent variability within hillslopes and different surface conditions caused by fire.
21	USA: Oregon and Washington, U.S.	R: Wagenbrenner et al. (2010) and Robichaud et al. (2010, 2007) D/M: Filed EXP/WEPP model	<ul style="list-style-type: none"> The disturbed sites have higher runoff rates, velocities, and sediment flux rates than the undisturbed sites. The sediment flux rates generally are greater in the initial stage of each runoff event than under the steady-state condition. Calculated rill erodibility increased by orders of magnitude with an increase in fire severity. The log-transformed stream power was the best hydraulic relationship for predicting sediment flux rates. <i>The rill erodibility values in a disturbed forest should not be held constant for a given rainfall-runoff event.</i>
22	USA: Potlatch River basin, north central Idaho, U.S./croplands	R: Teasdale and Barber (2008) D/M: High resolution aerial imagery	<ul style="list-style-type: none"> Seasonal high-resolution digital aerial imagery can be used to detect ephemeral gullies and analyze gully morphology.

Table 1 (continued)

#	Country: Location/Land-cover	Reference (R) Data/Model (D/M) Location/Land-cover (L/L)	Key results/limitations (or comments)
23	USA: The lower Snake River basin/forests, agricultural lands, and urban area	R: Tetra Tech EC, Inc. (2006) D/M: Inventory	<ul style="list-style-type: none"> • An erosion potential index (EPI) is developed with aerial imagery to identify agricultural fields with risk of ephemeral gully erosion at large watershed scales. • <i>The effects of winter hydrology should be included for the EPI method.</i> • There are limited data on major sediment sources and yields in the Snake River basin. • <i>A multi-year sediment transport monitoring program should be conducted.</i> • <i>An initial sediment budget estimate is needed.</i>
24	USA: Targeting ungauged rural basins throughout the US; tested over Oklahoma and Texas/rural area with cropland, rangeland and non-agricultural land	R: Williams et al. (1985) and Williams and Berndt (1977) D/M: Simulator for Water Resources in Rural Basins (SWRRB) and the Modified Universal Soil Loss Equation (MUSLE)	<ul style="list-style-type: none"> • A sediment routing model is added to MUSLE. • MUSLE uses runoff variables (i.e., runoff volumes and runoff peak flows), rather than rainfall erosivity, to estimate sediment yields so that it can give single storm estimates of sediment yields.
25	Australia: Sandstone Tablelands near Sydney/eucalypt forest	R: Doerr et al. (2006) D/M: Field OBS	<ul style="list-style-type: none"> • The model performs well when rainfall is generated. • High severity burns caused destruction of repellency in the surface soil layer. • <i>Existing fire severity classifications for predicting fire impacts on hydrologic responses need to be improved, which encompasses not only foliage and ground cover status, but also changes to surface and subsurface soil hydrologic properties.</i>
26	Australia: Eastern Victorian Uplands, near Melbourne/Mixed forests	R: Langhans et al. (2016) D/M: an intermediate model between physically-based/distributed and lumped/empirical; Monte-Carlo approach simulation	<ul style="list-style-type: none"> • This model can be used to assess risk to water quality due to fine sediment delivery after wildfire. • A fire spread model and an erosion model is coupled. • Headwaters, sub-catchments, and the water supply catchment are independent, but nested with rule-based linkages. • Fine sediment is most sensitive to the texture of source material, debris flow volume estimation, and the transmission of fine sediment estimates. • <i>Parameters and processes need to be calibrated when applied in other regions.</i>
27	Australia: Southeast Australian highlands (eastern uplands of Victoria)/from open dry forests, tall temperate rainforests, to Mountain Ash	R: Nyman et al. (2015) D/M: Erosion survey, aerial imagery, & logistic regression model	<ul style="list-style-type: none"> • Sediment yields from debris flows after wildfire are 2–3 orders of magnitude higher than background erosion rates. • Debris flow susceptibility was quantified with a logistic regression based on an inventory from 315 debris flow fans; burn severity (differenced normalized burn ratio, <i>dNBR</i>), local slope, dryness, and rainfall intensity are significant predictors. • Burn severity is an important control on sediment delivery. • A drier catchment might be more susceptible to debris flows than wetter regions.
28	Canada: Western Canadian mountainous catchments/Montane Spruce, etc.	R: Mahat et al. (2015) D/M: Conceptual modeling (HBV-EC)	<ul style="list-style-type: none"> • A reduced forest canopy cover after wildfire will likely cause early initiation of snowmelt and peak flow. • <i>Both pre-wildfire and post-wildfire data are needed for evaluating the impacts of wildfire on catchment hydrology with a conceptual modeling approach.</i> • <i>A more physically-based model is needed for evaluating wildfire impacts on hydrology when pre-fire data are unavailable.</i>
29	Canada: Rocky Mountains (Alberta)/Montane and subalpine ecozones	R: Silins et al. (2014) and Silins et al. (2009, 2008) D/M: Field OBS	<ul style="list-style-type: none"> • Sediment production increased dramatically in burned and post-fire salvage logged catchments, while they were strongly mediated by topography and hydro-climatic controls. • Post-fire salvage logging produced much greater impacts than wildfire alone. • The practice of post-fire salvage logging produces more sediment than burnt watersheds without salvage logging. • Wildfire and salvage logging could cause a cascading series of ecohydrologic effects on aquatic ecosystems through increasing mean annual concentrations of all forms of phosphorus (P), and the median, and the maximum of concentrations of total phosphorus (TP).
30	China: Daxing'an Mountains, Heilongjiang/coniferous forest	R: Cui et al. (2014) D/M: Field EXP	<ul style="list-style-type: none"> • The change in soil organic carbon (SOC) after wildfire depends on fire severity and topology/location: low- and medium-severity fires have no significant immediate effect on SOC; high-severity fires cause a large and immediate loss of C through direct combustion or high-temperature volatilization.

(continued on next page)

Table 1 (continued)

#	Country: Location/Land-cover	Reference (R) Data/Model (D/M) Location/ Land-cover (L/L)	Key results/limitations (or comments)
31	China: Hong Kong/Dicranopteris fern or bare ground	R: Hill and Peart (1998) D/M: literature review & Field EXP	<ul style="list-style-type: none"> • After burning, large quantities of sediment move on the slopes but this is short-lived because of the extremely rapid recovery of vegetation by mid-May. • While burnt plots generated 3–5 times more sediment yield from hillslopes than unburnt plots, there is a small difference in sediment levels in small streams; i.e., much of this additional yield is not delivered to the streams. • <i>There is a need for further research on the linkages between on-slope plot studies with catchment-level studies.</i>
32	Greece: Mediterranean/coniferous forests, woodland-shrubs, and croplands	R: Karamesouti et al. (2016) D/M: RUSLE and the Pan-European Soil Erosion Risk Assessment (PESERA)	<ul style="list-style-type: none"> • RUSLE shows high sensitivity to topographic and rainfall erosivity; while PESERA is more sensitive to vegetation coverage as well as to soil characteristics. • RUSLE modeled significantly higher erosion rates over both pre- and post-fire settings. • <i>Experimental measurements are required for evaluating model performance.</i>
33	South Korea: Gangneung/pine trees	R: Shin et al. (2013) D/M: Field/Catchment EXP	<ul style="list-style-type: none"> • The runoff coefficient has a high correlation with rainfall amount, while the sediment response rate is highly controlled by vegetation structure, litter, and root. • The sediment response rate decreased greatly within two years after wildfire with vegetation recovery. • Stream-head hollows function as areas of deposition rather than erosion, unless disturbed by heavy rainfall events and landslide processes.
34	USA: Salmon River Basin (the central of Idaho)/forest, shrubland, herbland, and cropland	R: This study D/M: coupled VIC and WEPP-HE	<ul style="list-style-type: none"> • We model the effects of climate change and extreme wildfire activity on erosion at the basin scale. • A hillslope-scale erosion model was nested into a macro-scale hydrologic model. • Wildfire exacerbates the impacts of climate change on the hydrograph shape. • Climate change may exacerbate the impacts of extreme wildfires on sediment yield. • <i>More field observations and experiments are needed to evaluate model performance.</i> • <i>Vegetation regrowth after fire should be explicitly simulated.</i>

^a Abbreviation for "observation".

^b Abbreviation for "experiment".

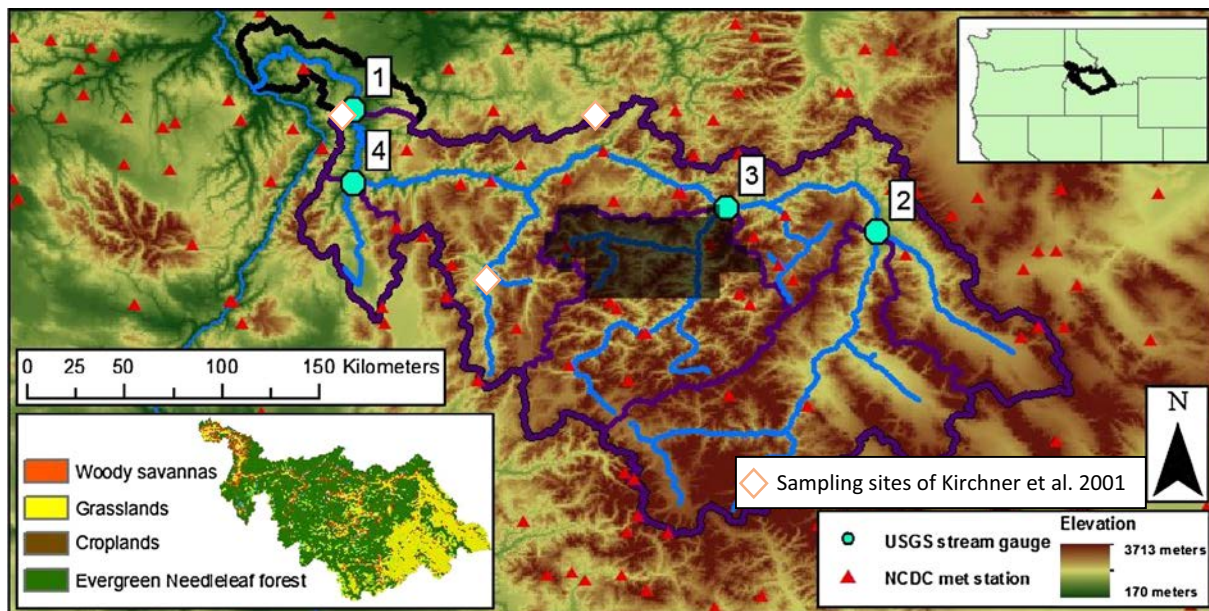


Fig. 1. Salmon River basin map showing calibration basins in purple (with basin number reference), elevation, land cover, National Climate Data Center (NCDC) stations, and test area (shaded).

(Sridhar et al., 2013; Tang et al., 2012). WEPP-HE is a stand-alone process-based erosion model that has been extracted from the full WEPP model (v2004.7) which operates over field and hillslope scales (hundreds of m²) for specific storm events (Flanagan et al., 2005; Mao et al., 2010). Linking of these two models (that operate at different temporal and spatial scales) requires spatial and temporal disaggregation of VIC output prior to running WEPP-HE. To reduce computation time, WEPP-HE was run using the representative hillslope approach (as described below) and erosion results are aggregated over each hillslope class subsequent to analysis.

We followed the same procedures as Mao et al. (2010) to perform VIC model simulations, to transform VIC model outputs to drive WEPP-HE, and to aggregate WEPP-HE simulated results to the level of the VIC model grid cell. Because methodologies related to these pre- and post-processes have been described in detail by Mao et al. (2010), here we focus on the differences in how we implemented the VIC-WEPP model, including our refinements for post-fire applications. This process involved three major steps, as follows.

1. For each VIC model grid cell, the VIC model passes hydrologic information (runoff depth, peak runoff rate, effective runoff duration, and effective rainfall intensity and duration) to WEPP-HE. This step involves a rainfall disaggregation step, as described by Mao et al. (2010). See further details in Section 3.2 on meteorological data sources.
2. We select representative hillslopes in each VIC grid cell by using a stratified sampling scheme (Park and van de Giesen, 2004; Thompson et al., 2006) to perform simulations from each relatively homogeneous subgroup (e.g., with similar slope gradient ranges) and from each vegetation cover. The number of representative hillslopes selected for each subgroup is set proportionally by the fractional areal coverage within the grid cell. The slope distribution in each VIC model grid cell is downscaled from a 500-m DEM data with a monofractal scaling method, which is based on the monofractal nature of topography (Klinkenberg and Goodchild, 1992; Xu et al., 1993; Zhang et al., 1999), i.e. topography estimated from a DEM is a function of the pixel size and the slope gradient is linked with the fractal dimension of the topography. This method has been used and evaluated by Bowling et al. (2004) and Mao et al. (2010) to downscale 30 arc second DEM to 50 m and 30 m resolution slope, respectively. We identified five slope ranges as <20°, 20–36°, 36–52°, 52–70°, and >70°, over which the number of sampled hillslopes covers 22.7%, 27.8%, 22.4%, 14.9%, and 12.2% of total hillslopes in the SRB, respectively.
3. Soil information, beyond what is needed for VIC modeling, is gathered; these include baseline erodibility, soil particle size classes, size class specific gravity, and organic matter content. Erodibility adjustments (due to ground cover, canopy effects, live and dead root biomass, and residue) are handled in the coupled model using a variety of relationships that were developed by Mao et al. (2010). New erodibility adjustments are made to

account for the effects of wildfire, as follows. Five vegetation and soil parameters are identified to be adjusted for post-fire conditions with three various fire severities (i.e. low fire, moderate fire, and high fire): leaf area index (*LAI*), saturated hydrologic conductivity (K_c), interrill erodibility (K_i), rill erodibility (K_r), and critical shear stress (τ_{crit}) (Parson et al., 2010; Robichaud, 2000; Robichaud et al., 2007). *LAI* adjustment factors for low, moderate, and high fire severity conditions are taken from Parson et al. (2010) (Table 2). K_c for low and high fire severities were from Robichaud (2000) and the value for the moderate fire severity is the average of the low and high fire conditions. *LAI* and K_c adjustments are applied for both VIC (for hydrological processes) as well as WEPP-HE (for soil erosion processes) simulations. Initial values of K_i , K_r , τ_{crit} and their adjustments for different fire severities are identified using the WEPP soil database (Frankenberger et al., 2011) and for pre- and post-fire conditions for forests from Robichaud et al. (2007). The averages of these two data sources are used for this study and the parameters for moderate fire severity are calculated as the average of low and high fire conditions (Table 2), although the τ_{crit} parameter does not change with low and high fire conditions according to Frankenberger et al. (2011) and Robichaud et al. (2007). The values for the sandy loam conditions (i.e. 55% sand, 35% silt, and 10% clay) are selected from these two data sets because of this soil type's dominance over the SRB. In our sensitivity analysis we assume uniform fire severities everywhere in the SRB under each fire severity scenario. This is a sensitivity study around the worst case scenario, as wildfires in reality have not occurred simultaneously over such a large spatial extent. According to the Global Fire Emissions Database (GFEDv4) (Randerson et al., 2015), during the period of 1997 to 2014, the 25 to 75th percentile of burnt area in the SRB ranged between 53.6 and 411.9 km² (or 0.15–1.14% of total land area).

3.2. VIC model input data

Historical gridded meteorological data were necessary for model evaluation and for providing baseline estimates for the future climate scenarios. We use the dataset created by Abatzoglou (2013) which covers a period of 1979 to 2010, and includes daily precipitation, air temperature, and wind speed. Abatzoglou statistically downscaled the data from the North American Land Data Assimilation System Phase 2 (NLDAS-2, (Mitchell et al., 2004)) to 1/24th degree (~4-km) resolution by using data derived from the Parameter-elevation Regressions on Independent Slopes Model (PRISM, (Daly et al., 2008)). For future climate simulations, we use a dataset created by Abatzoglou and Brown (2012), who statistically downscaled and bias-corrected future daily gridded climate data (from 2039 to 2070) from the Coupled Model Intercomparison Project Phase 5 (CMIP5) using the Multivariate Adapted Constructed Analogs (MACA) method. These spatially downscaled climate data are suitable for this study as MACA

Table 2
Adjustment factors for key post-fire erosion parameters as implemented in the VIC and WEPP-HE models.^a

Parameter	Adjustments (within the parentheses is the value)			
	No fire	Low fire	Moderate fire	High fire
<i>LAI</i>	1	0.6	0.25	0.05
K_c	1	0.9	0.775	0.65
K_i (kg s m ⁻⁴)	1 (400,000)	1.75 (700,000)	2 (800,000)	2.25 (900,000)
K_r (s m ⁻¹)	1 (0.00027)	1.887 (0.0005)	2.075 (0.00055)	2.264 (0.0006)
τ_{crit} (N m ⁻²)	1 (1.5)	1 (1.5)	1 (1.5)	1 (1.5)

^a Abbreviations: *LAI*: leaf area index; K_c : saturated hydrologic conductivity, K_i : interrill erodibility, K_r : rill erodibility, and τ_{crit} : critical shear stress.

conserves the relationships between meteorological variables and has been shown to closely follow extreme fire danger metrics (Abatzoglou and Brown, 2012). All 1/24th degree gridded climate data were aggregated into 1/16th degree resolution for running the VIC model.

The soil and vegetation parameters for VIC model simulations are from Hamlet et al. (2013) that include new calibrations based on Elsner et al. (2010). Soil types and physical properties are originally derived from the State Soil Geographic (STATSGO) database (Kirschbaum and Lettenmaier, 1997; Nijssen et al., 1997; United States Department of Agriculture, 1994). The land cover type is reclassified from MODIS MOD 12Q1 data with 500-m resolution (Friedl et al., 2002). The 500-m resolution digital elevation model (DEM) data are from the Global Multi-resolution Terrain Elevation Data 2010 (GMTED2010) (Danielson and Gesch, 2011).

3.3. Model calibration

Four U.S. Geologic Survey (USGS) streamflow gauging stations are used for model calibration and evaluation (see Fig. 1 and Table 3). Three of these stations are at the outlet of independent watersheds (stations 2–4), while one is at the outlet of the entire SRB (station 1) (Table 3). VIC model calibration parameters include the variable infiltration curve parameter (b_i [-]), maximum velocity of baseflow (D_{smax} [mm day⁻¹]), fraction of maximum velocity of baseflow (D_s [-]) and fraction of maximum soil moisture (W_s [-]) where non-linear baseflow begins, depth of second (D_2 [m]) and third soil layers (D_3 [m]), and snow surface roughness ($Snow_{-rough}$ [m]) (Gao et al., 2010). A streamflow routing process (Route 1.0) is conducted for comparing simulated daily runoff with stream hydrograph (Lohmann et al., 1998, 1996). Observations from these four gauges are also used for model evaluation, but over independent periods. Calibration is first conducted using stations 2–4, then the parameters for the remaining parts of the SRB are calibrated to match the observed streamflow at station 1.

In addition to calibration of the soil parameters, we also bias-correct the simulated incoming shortwave radiation from the VIC meteorology sub-module, which uses the algorithms of the Mountain Microclimate Simulation Model (MT-CLIM; (Hungerford et al., 1989; Kimball et al., 1997; Thornton et al., 2000; Thornton and Running, 1999)) to estimate shortwave radiation from the daily temperature range and other variables. Barsugli et al. (2012) and Bohn et al. (2013) indicate that MT-CLIM may generate substantial biases over interior continental regions in the presence of snow, such that the adjustments are needed to eliminate biases in the timing of snowmelt.

In addition to matching the shape of the average monthly hydrograph during calibration periods, the Nash-Sutcliffe efficiency (NS) metric (Eq. (1)) is used to evaluate simulated streamflow against the gauge observations during model evaluation periods (Table 3).

$$NS = 1 - \frac{\sum_{i=1}^n (O_i - P_i)^2}{\sum_{i=1}^n (O_i - \bar{O})^2} \quad (1)$$

Here, \bar{O} is the observed mean streamflow, O_i is the observed streamflow, and P_i is the simulated streamflow for each time step, i . For a perfect model, NS would be one while Moriasi et al. (2007) suggest that model performance can be thought as acceptable if NS is greater than 0.60 at daily time-steps.

3.4. Model evaluation

3.4.1. Streamflow

For evaluation of the model's performance beyond the calibration period, the following additional metrics are calculated: daily peak flow (PK) (Eq. (2)), averaged yearly relative bias (RB) (Eq. (3)), and daily and monthly root-mean-square error ($RMSE$) (Eq. (4)). PK emphasizes the model's capability in estimating daily extreme events, wherein a PK value ranging 0.1–0.15 can be thought of as good model performance (a perfect model would yield a zero PK) (Coulibaly et al., 2001). PK is calculated as

$$PK = \frac{\left[\sum_{i=1}^{n_p} (Q_{pi} - \hat{Q}_{pi})^2 (Q_{pi})^2 \right]^{\frac{1}{4}}}{\left(\sum_{i=1}^{n_p} (Q_{pi})^2 \right)^{\frac{1}{2}}} \quad (2)$$

where n_p is the number of peak flows greater than one-third of the observed average daily peak streamflow, Q_{pi} is the observed daily flow, and \hat{Q}_{pi} is the simulated daily streamflow (Coulibaly et al., 2001). RB , on the contrary, emphasizes the simulation accuracy on annual streamflow rather than daily extremes, as follows

$$RB = \frac{\sum_{i=1}^{n_y} (P_i - O_i) / (O_i)}{n_y} \quad (3)$$

where n_y is the number of years, P_i is the simulated streamflow, and O_i is the observed streamflow, for each year, i . $RMSE$ is used to quantify biases of modeled daily or annual streamflow over the simulation period, as follows

$$RMSE = \sqrt{\frac{\sum_{i=1}^{n_m} (P_i - O_i)^2}{n_m}} \quad (4)$$

where n_m is the number of months or days, P_i is the simulated result, and O_i is the observation.

3.4.2. Sediment yields

In addition to evaluating simulated streamflow, we also compare simulated sediment yields against a long-term average measured sediment yield from the SRB by Kirchner et al. (2001). Kirchner et al. (2001) measured erosion rates over long temporal scales (6300–26,000 years) using cosmogenic ¹⁰Be, and over shorter scales (short-term; record lengths of 10–28 years) using conventional sediment-trapping and sediment-gauging methods. Because slope and land cover type were not specified for each specific sample location by Kirchner et al. (2001), the VIC-WEPP model sediment yields that are compared are from the model grid cells that the catchment boundaries of Kirchner et al. (2001) falls within. Although the spatial scales of the model and the catch-

Table 3
USGS gauges for model calibration and evaluation.

Watershed	Gauge station name	Period for calibration	Period for evaluation	Drainage area [km ²] (% of total calibration area)
1	Salmon River @ White Bird, ID	Jan. 1979 – Dec. 1994	Jan. 1995 – Dec. 2010	34,760 (100%)
2	Salmon River @ Salmon, ID	Jan. 1979 – Dec. 1994	Jan. 1995 – Dec. 2010	9679 (27.8%)
3	Middle Fork Salmon River @ Mouth NR Shoup, ID	Oct. 1993 – Mar. 2002	Apr. 2002 – Sep. 2010	7449 (21.4%)
4	Little Salmon River @ Riggins, ID	Jan. 1979 – Dec. 1994	Jan. 1995 – Dec. 2010	1491 (4.3%)

Table 4

Vegetation type and cover fractions used in Disturbed-WEPP and the VIC-WEPP model.

VIC-WEPP Vegetation	Disturbed-WEPP		
	Vegetation	%Cover	%Rock
Forest	5 year old forest	100	20
Wooded grassland	Tall grass	80	20
Prairie	Short grass	50	20
Cropland	Tall grass	40	20
Other types	high severity fire	1	40

ments from Kirchner et al. (2001) are different and only seven catchments are available in the SRB (Fig. 1), an evaluation provided the general order of magnitude difference between the VIC-WEPP model and observed yields.

3.4.3. Model inter-comparison

For placing our simulated results in context of existing and frequently-applied tools, the VIC-WEPP model simulated results are compared against hillslope-level WEPP simulations using the Disturbed-WEPP (v2010.01) web-based tool, which is designed to capture the effects on erosion due to multiple types of disturbances in forest and rangeland ecosystems and is often used for informing land management decisions (Elliot and Hall, 2010). Ten grid cells (located in the western half of the SRB), of which each contains 96–199 sampled hillslopes, are selected for running both models with two fire severity scenarios: no fire and high fire. The same climate (which were generated using a rainfall disaggregation process), slope, and soil texture data are used in both models. The default vegetation definitions are different in these two models; therefore, when running Disturbed-WEPP, we adjust the default values of % cover and % rock to describe the corresponding VIC-WEPP model vegetation type (Table 4) (Elliot and Hall, 2010). For comparison purposes, we average erosion results from the no-fire and high-fire scenarios from VIC-WEPP and compared these results to those from Disturbed-WEPP.

3.5. Future climate scenarios

To quantify the impact of climate change on streamflow over the SRB, we select five future climate scenarios out of the 24 scenarios that are available to us by Abatzoglou and Brown (2012). The 24 scenarios include twelve different General Circulation Models (GCMs) for each combination of two Representative Concentration Pathways (RCP4.5 and RCP8.5). The five scenarios were identified to cover the range of possible projected annual precipitation and temperature changes over the basin, which were calculated as percent change and absolute difference, respectively, between the periods of 1979–2010 and 2039–2070 (Table 5; Fig. 2).

For simulating the impacts of climate change on sediment yield from the entire SRB, we chose downscaled climate data from MIROC5 only (the mid-range future climate scenario), due to the

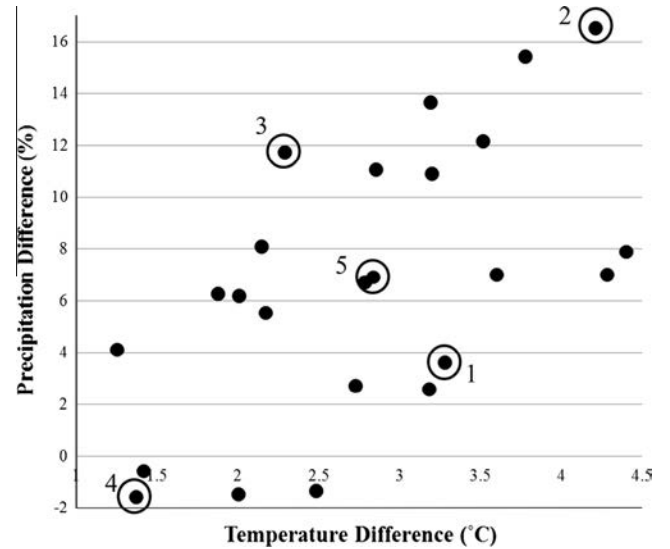


Fig. 2. Selection of the future climate scenarios for analysis (among 24 CMIP5 scenarios available to us by Abatzoglou and Brown, 2012) was performed by selecting the four corners plus the middle scenario when plotting them in terms of projected annual precipitation and temperature changes over the basin.

large computational requirements of the WEPP-HE model. To assess the effects that the uncertainty of future climate scenarios has on sediment yield, we ran all five scenarios over a selected test area (see gray area in Fig. 1). This test area covers 80 grid cells and is a good representation of the entire SRB in terms of ranges of annual precipitation, slope, land cover, and estimated sediment yield change.

For both historical and future simulations, we remove the first two years of simulated results to allow for model spin-up. Therefore, when analyzing results, we utilize the 30-year average periods of 1981–2010 and 2041–2070 for historical and future simulations, respectively.

4. Results

4.1. Calibration and evaluation

Over the calibration periods, all selected watersheds have *NS* larger than 0.6 on both daily and monthly simulated streamflow except Watershed-2 (for which *NS* equals 0.4 and 0.56 for daily and monthly time steps, respectively) (Table 6). Over the SRB as a whole, the calibrated VIC model successfully captures the timing of peak flow and the daily and monthly magnitudes during the calibration period (Fig. 3). The *PK* values for all watersheds are less than the criteria identified by Coulibaly et al. (2001); this indicates that the model captures peak flows relatively well (Table 6). All *RB* values from these four watersheds are less than 15%, while Watershed-3 has the least bias of -0.3% (Table 6). The *RMSE*

Table 5

Selected GCMs (General Circulation Models) and RCPs (Representative Concentration Pathways) for VIC-WEPP model simulations over the period of 2039–2070.

Model #	Model and version	Institute	RCP scenario
1	BCC_CSM1.1	Beijing Climate Center, China Meteorological Administration, China	8.5
2	CanESM2	Canadian Centre for Climate Modeling and Analysis, Canada	8.5
3	GFDL-ESM2G	US Department of Commerce/NOAA/Geophysical Fluid Dynamics Laboratory, USA	8.5
4	INMCM4.0	Institute for Numerical Mathematics, Russia	4.5
5	MIROC5	Atmosphere and Ocean Research Institute (The University of Tokyo), National Institute for Environmental Studies, and Japan Agency for Marine-Earth Science and Technology, Japan	4.5

Table 6
Calibration and evaluation metrics over selected watersheds (see Fig. 1 for streamflow gauging locations). While NS was calculated separately for both the calibration and evaluation periods, PK, RMSE, and RB were calculated for the evaluation periods only.

Watershed	NS (calibration period)		NS (evaluation period)		PK	RMSE [$\text{m}^3 \text{s}^{-1}$]		RB
	Daily	Monthly	Daily	Monthly		Daily	Monthly	
1	0.88	0.96	0.83	0.93	0.095	162	884	-0.098
2	0.41	0.56	0.59	0.81	0.108	34.6	187	0.148
3	0.60	0.83	0.71	0.90	0.124	52.5	279	-0.003
4	0.76	0.93	0.75	0.88	0.099	14.0	75.1	-0.103

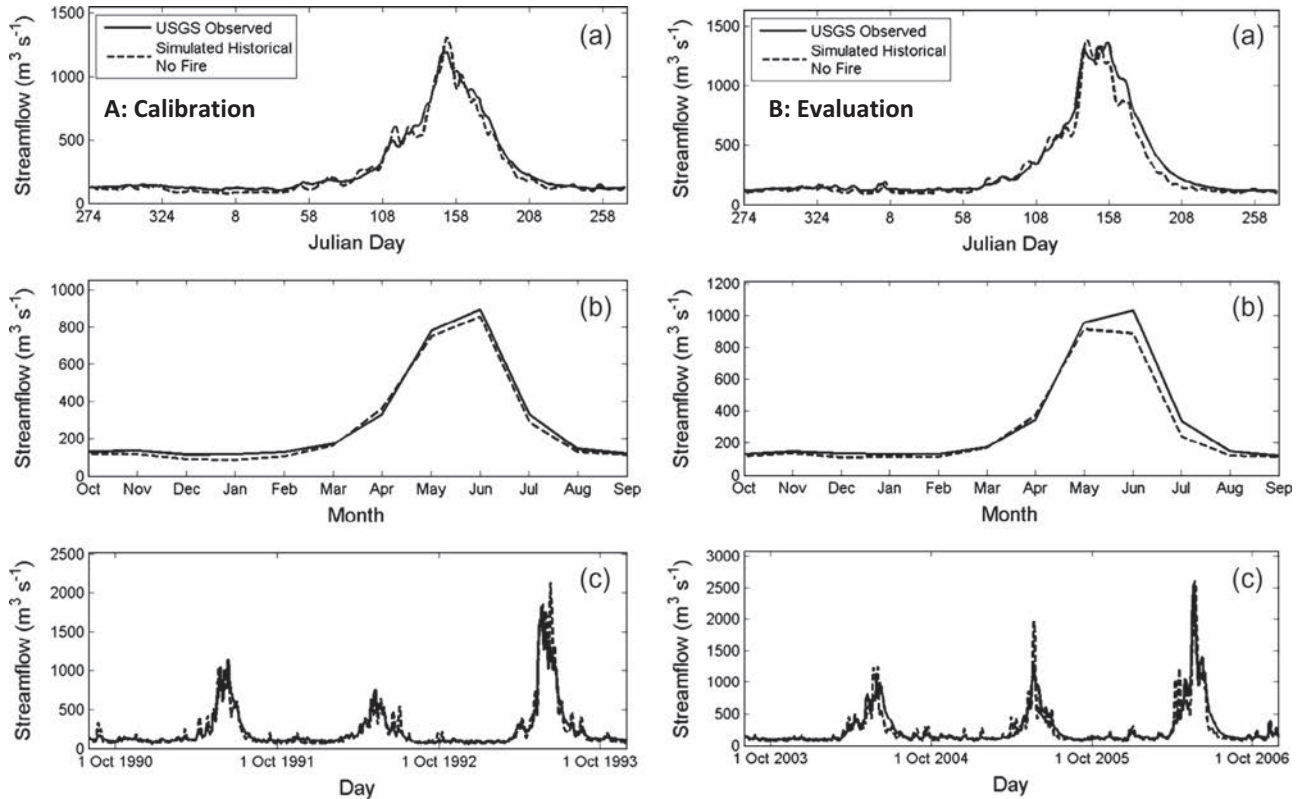


Fig. 3. Observed and simulated discharge over the calibration (A) and evaluation (B) periods at the outlet of the SRB (station #1 in Fig. 1) for (a) the average Julian day, (b) average month, and (c) three years of daily flows. The “averages” are the mean value during the calibration and evaluation periods for panel A and panel B, respectively.

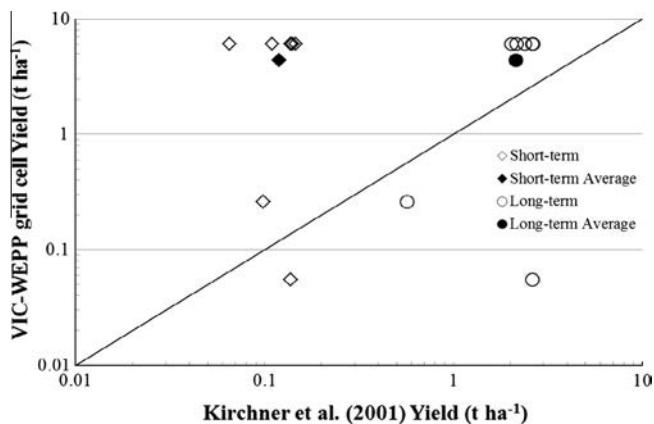


Fig. 4. Comparisons of average annual sediment yield between the VIC-WEPP simulated results and short-term and long-term observations from Kirchner et al. (2001).

depends on the magnitude of average streamflow so that it is expected that Watershed-1, the entire SRB, has the largest bias in absolute value from the observations [Table 6].

The average VIC-WEPP sediment yield from the seven SRB sites (Fig. 4) is 4.37 t ha^{-1} , while the average yield from Kirchner et al. (2001) over the short-term and long-term scales are 0.12 and 2.14 t ha^{-1} , respectively (Fig. 4). Because of the naturally episodic pattern and the underestimation of short-term soil erosion from conventional sediment-yield data (Kirchner et al., 2001), the difference in measured versus simulated erosion estimates do not lead us to believe that there are major (order of magnitude) biases in simulated erosion rates. VIC-WEPP modeled results over catchments with long-term high-potential sedimentation yields are close to measurements, even though there are some bias over catchments with relatively low-potential erosion (Fig. 4). This indicates that the VIC-WEPP model is particularly suitable for estimating long-term average sediment yields.

4.2. Model inter-comparison and model sensitivities to various parameters

The VIC-WEPP model and Disturbed-WEPP predicted an average annual sediment yield of 0.85 and 0.36 t ha^{-1} , respectively. While the VIC-WEPP model yields were on average more than double that from Disturbed-WEPP, the VIC-WEPP model generated

a much larger dynamic range of sediment yield estimates from individual hillslopes (from 0 to 125 t ha^{-1}) as compared to Disturbed-WEPP (from 0.01 to 10 t ha^{-1}) (Fig. 5). While Fig. 5 would suggest that the basin-average yield would be lower for VIC-WEPP, the higher yield estimates that exceed the dynamic range of Disturbed-WEPP simulations ($>10 \text{ t ha}^{-1}$) result in an overall higher sediment yield. The difference in results between these two models arises from differences in input parameters (i.e., we were able to provide detailed input parameters to the VIC-WEPP model but utilized default parameters when running Disturbed-WEPP) as well as from different sensitivities to each of these parameters (Table 7).

For Disturbed-WEPP, the differences in average annual precipitation have the largest effects on yield followed by slope length and slope (Table 7). For the VIC-WEPP model, the land cover type is most influential on erosion followed by slope length, slope, and precipitation. Disturbed-WEPP is more sensitive than the VIC-WEPP model to hydraulic conductivity, τ_{crit} , and K_r ; while the VIC-WEPP model is more sensitive to changes in land cover, average annual precipitation, slope length, and slope.

4.3. Climate change and fire impacts on streamflow

Under the no-fire scenario, future climate change will decrease SRB peak streamflow and shift it earlier in the season (Fig. 6). The

magnitude of peak streamflow in a future climate increases with higher fire severity scenarios until it becomes larger than the historical peak streamflow under the no-fire scenario (Fig. 6). Under the low and moderate fire severity scenarios, the projected timing of peak streamflow has a small earlier shift (~ 15 days) from the historical period. However, under the high-fire scenario, the occurrence of peak streamflow is shifted much earlier with respect to the other lower fire severity scenarios in a future climate, and is around 50 days earlier than the historical no-fire scenario (Fig. 6). The shifting of peak streamflow is mostly controlled by the warming-induced early snowmelt (Hamlet et al., 2013; Mote et al., 2005). The increase in peak flow magnitude with increasing fire severity is due to less vegetation available to store water and the surface being more repellent due to wildfire which caused an increase in runoff. The decreased vegetation and increased surface repellency is caused by the changes in the post-fire adjustment factors LAI and K_c for each fire severity condition. Over three smaller watersheds within the SRB, climate change and fire severity result in similar impacts to the magnitude and timing of peak streamflow (results not shown). We note that in Fig. 6 we assume that the entire SRB has the same fire treatment for each of the wildfire scenarios. This does not represent a realistic situation (most individual fires will in reality burn only a portion of the watershed) but provides for a worst case scenario that we use to examine relative sensitivity between climate and wildfire impacts on runoff and erosion.

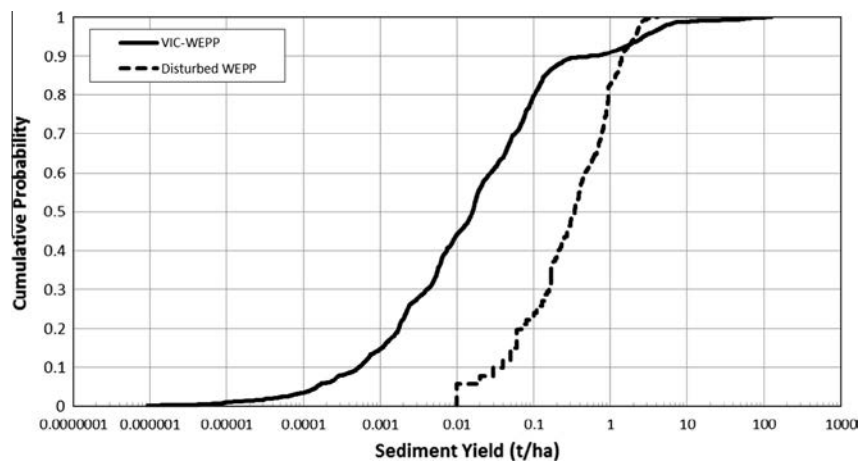


Fig. 5. Cumulative Distribution Functions (CDFs) of estimated average annual sediment yields over all hillslopes from the VIC-WEPP and Disturbed-WEPP models.

Table 7

Range of input parameters for the two contrasted models (Disturbed WEPP and VIC-WEPP), and the sensitivity of sediment yield to model parameters (expressed both as an absolute magnitude and as a relative sensitivity).

Parameter	Disturbed WEPP			VIC-WEPP		
	Range	Yield Change (t ha^{-1})	Rate of yield change (fraction)	Range	Yield change (t ha^{-1})	Rate of yield change (fraction)
Annual precipitation (mm)	598–1296	9.56	0.0137	598–1296	10.2	0.0146
Slope (%)	1–100	5.00	0.051	1–100	21.0	0.191
Slope length (m)	5–95	7.10	0.079	5–95	–12.6	–0.140
Hydraulic conductivity (mm day^{-1})	144–672	–0.64	–0.0012	300–2700	–0.125	–0.0001
Cover (%)	0–100	–0.50	– ^a	–	–	–
Critical shear (τ_{crit}) (N m^{-2})	0.5–1.0	–0.41	–0.82	0.45–1.05	–0.013	–0.02
Rill erodibility (K_r) (s m^{-1})	0.0003–0.0004	0.07	700	0.0001–0.0007	0.00	0.00
Land cover	–	–	–	Forest, Wooded grassland, Prairie, Cropland, and Bare soil	2051	–
LAI (fraction)	–	–	–	0.4–1.6	–2.1	–
Interrill erodibility (K_i) (kg s m^{-4})	–	–	–	300,000–1,500,000	5.08	–

^a Indicates the parameter was not used in the specific model sensitivity test.

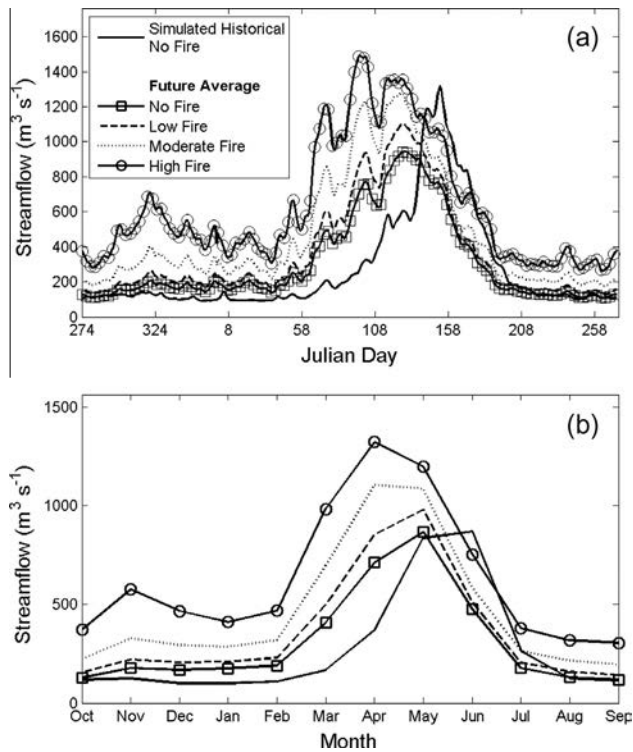


Fig. 6. Simulated mean (a) daily and (b) monthly streamflow from the outlet of the SRB in the future (i.e. 2041–2070) under different fire severity conditions (i.e. no, low, moderate, and high). The future streamflows shown (for each fire scenario) are the average of streamflow simulations for the five selected climate scenarios. Also shown, for comparison, is historical climate streamflow under the no-fire scenario.

Allowing the entire basin to burn provides insight as to which portions of the watershed are most sensitive to fire-induced erosion.

4.4. Climate change and fire impacts on sediment yield

Climate change and fire conditions both have significant effects on the generation of sediment over the SRB, but their impacts are different in terms of both magnitude and spatial variability. Our model results indicate that increases in fire severity will substantially increase sediment yield across the entire SRB under both historical (+26.0 t ha⁻¹) (Fig. 7a) and future (+31.2 t ha⁻¹) climate scenarios (Fig. 7b); however, the increases mainly occur from the forested lands in the central and western parts of the basin (Fig. 7a and b). The effects of climate change (versus from fire conditions) on soil erosion are more heterogeneous across the basin. Under the no-fire condition, climate change will result in a modeled decrease (increase) of yield over the central (eastern) portions of the SRB. On average for the entire basin, climate change (for the mid-range climate scenario, MIROC5 RCP4.5) will decrease soil erosion by 1.45 t ha⁻¹ (Fig. 7c). The mid-range climate scenario projects a moderate change in temperature and precipitation across most of the basin, but with more significant decreases in precipitation over the western SRB (results not shown), explaining the decrease in modeled yield due to climate change over that area. The increased sediment yield over the eastern part is because of the increased total precipitation and the increased fraction of precipitation as rainfall during winter and spring seasons caused by warming temperatures and the decrease of snowpack accumulation over this region. Under the high-fire scenario, most of the SRB will experience higher sediment yield in the future with an average yield increase of 3.7 t ha⁻¹ (Fig. 7d) and the effect of climate change will be small as compared to fire effects under the high-fire condition.

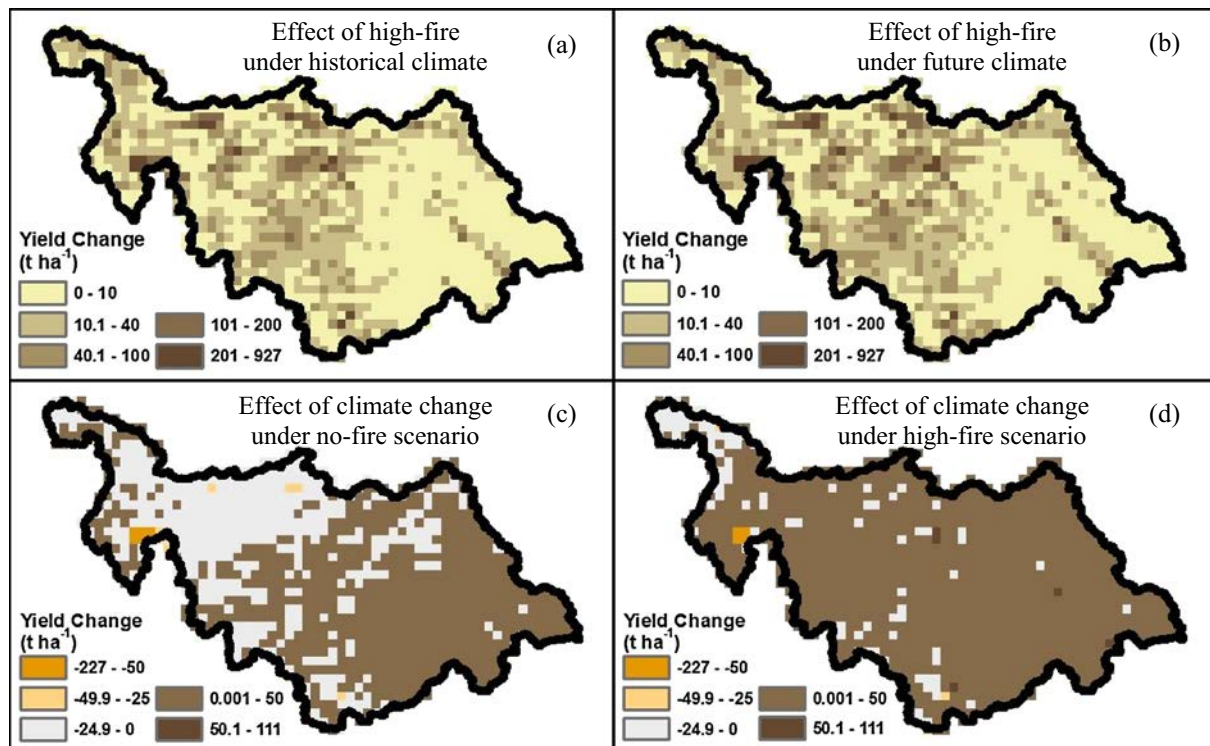


Fig. 7. Impacts of climate change and fire severity on sediment yield over the Salmon River Basin. Panels a and b depict the effects of fire severity during the historical (1981–2010) and future (2041–2070) periods, respectively. Panels c and d depict the effects of climate change under no-fire and high severity fire conditions, respectively. The magnitudes of changes in estimated sediment yield is calculated either by the differences between the high severity fire condition and the no fire condition under different climate scenarios (for a and b), or by the difference between future and historical climates while under different fire conditions (for c and d).

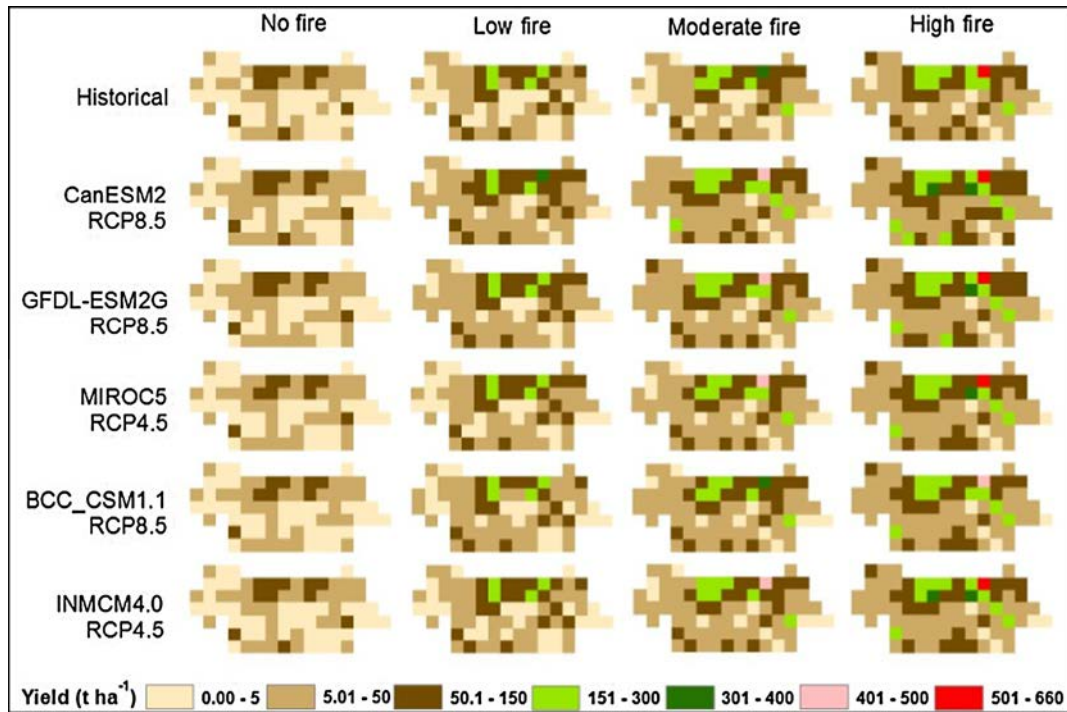


Fig. 8. VIC-WEPP simulated sediment yield for six climate and four fire severity scenarios over a portion of the Salmon River Basin (see gray area in Fig. 1). Historical and future yields are averaged over the periods of 1981–2010 and 2041–2070, respectively. The future climate scenarios are organized from top to bottom in order of larger to smaller increases in annual precipitation.

4.5. Model sensitivities to multiple climate projections

The five different future climate scenarios result in very similar patterns of sediment yield over the test area and for each of the fire scenarios (Fig. 8). While the impacts of climate change on sediment yield are much less than those of increasing fire severity (Fig. 9), isolation of the impacts due to individual climate scenarios uncovers differences in spatial heterogeneity that result from future climate uncertainty (Fig. 10). However, this uncertainty in response to climate change is at least an order of magnitude less than that associated with fire conditions.

5. Discussion

5.1. Implications

This modeling study suggests that the effect of fire severity is more important than the direct effect of climate change (through changes in temperature and precipitation) on sediment yield. This conclusion is consistent with earlier studies that highlight the controlling effects of wildfire severity on sediment yield and runoff (Table 1; e.g. Doerr et al., 2006; Elliot, 2013; Elliot and Hall, 2010; Helvey, 1980; Robichaud, 2000). However, we do not account for the indirect effects of climate change on soil erosion through its potential role in changing wildfire occurrence and severity; accounting for this indirect effect would likely accentuate the contribution of climate change to erosion. Recent studies have demonstrated that warming may result in heightened global aridity (by increasing atmospheric demand for moisture and altering atmospheric circulation patterns; Dai, 2011) and an earlier spring snowmelt (Mote et al., 2005). These effects can increase the length of the fire season and the extent of burnable area (Goode et al., 2012; Jolly et al., 2015; Westerling et al., 2006), although forest management practices and policies around fire suppression play an important if not dominant role in wildfire risk (Stephens and Ruth, 2005).

The climate sensitivity of sediment yield is in part due to warming-induced changes to the snowpack. While precipitation as compared to temperature acts as a stronger direct control on erosion, future precipitation projects are less certain. Therefore, impacts related directly to warming have a higher likelihood. An increase in the fraction of annual precipitation falling as rain and a longer snow-free season (due to a later accumulation and earlier melt) could increase the potential for sediment generation by increasing the exposure of the soil to rain droplets and increasing the length of the season during which overland runoff occurs. As a decreasing snowpack and earlier snowmelt have already been observed over the western U.S. and is projected to become more extreme (e.g. Adam et al., 2009; Elsner et al., 2010; Hamlet et al., 2013; Mote et al., 2005; Mote and Salathe, 2010), the impacts of snowpack changes on sediment yield potential and the subsequent impacts on water quality should be included along with assessment of the impacts of warming on water quantity, which are better understood (e.g. Hamlet et al., 2013; Liu et al., 2014; Tetra Tech EC, Inc., 2006). The role of the snowpack in the interplay between climate change and wildfire also needs further exploration as wildfire could lead to more exposure of the snowpack to sunlight because of a decreased canopy cover, as well as a decrease in snow albedo through black carbon, both of which can accelerate the snowmelt process and further impact sediment yields over burnt areas (Mahat et al., 2015).

5.2. Study uncertainties and limitations

Not accounting for the transient effects of fires on streamflow and erosion is a source of uncertainty in this study. We applied historical fire severity conditions to parameterize the entire SRB without addressing changes in future fire behavior (frequency or severity) or plant regrowth after a fire. Fire events were prescribed over the entire watershed. While we did this intentionally to examine the heterogeneity over the watershed of runoff and sediment yield response to changes in wildfire severity, this does not

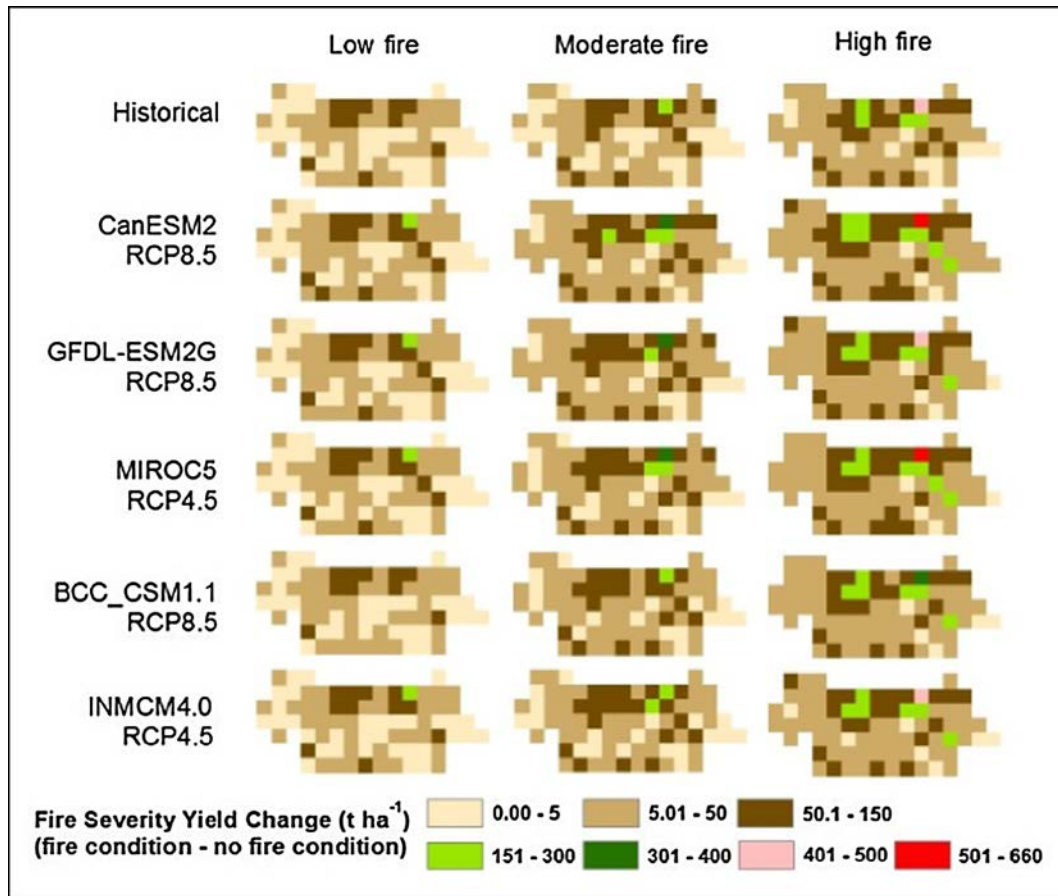


Fig. 9. Change in VIC-WEPP simulated sediment yield between three fire severities and the no fire scenario for six climate over a portion of the Salmon River Basin. See Fig. 8 caption for further details.

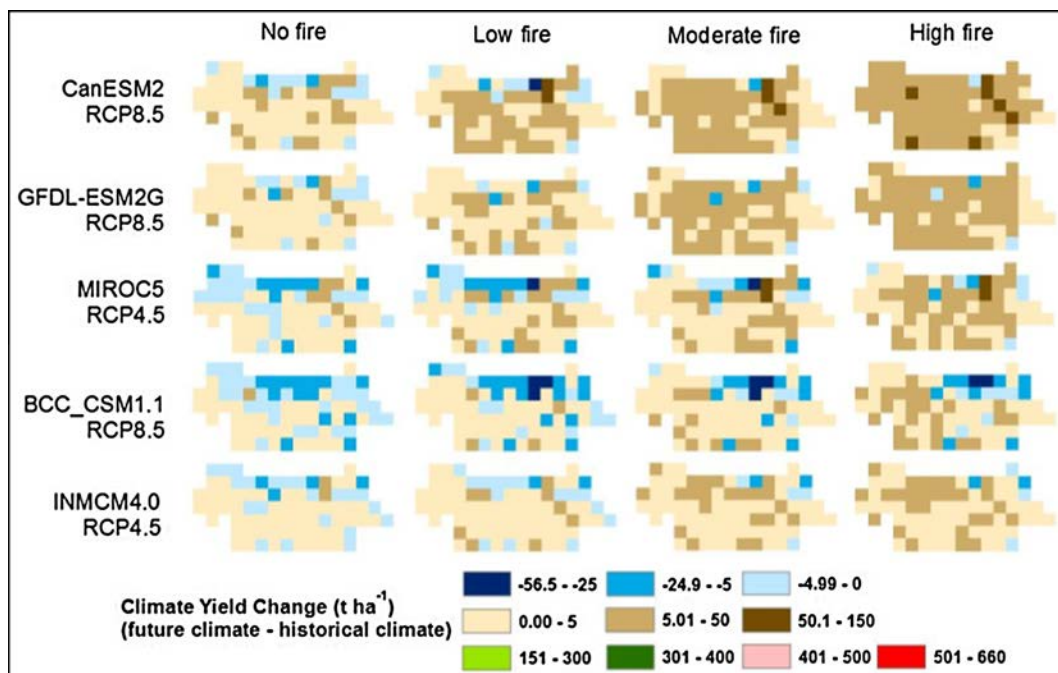


Fig. 10. Change in VIC-WEPP simulated sediment yield between five future climates and the historical scenario for four fire scenarios over a portion of the Salmon River Basin. See Fig. 8 caption for further details.

result in a realistic response at the basin scale. The results most affected by this limitation were the streamflow responses to wildfire because streamflow is an aggregate hydrologic process. Sediment yield results that were presented on a per area basis are less impacted by this limitation. Land cover and land use changes both historically and in the future were also not accounted for. Future studies should explore the transient behavior of climate and wildfire impacts on runoff and erosion.

As Kirchner et al. (2001) indicate, catastrophic erosion events might dominate the long-term sediment yield even though they are rare and brief. VIC–WEPP provides estimates of sediment yield due to runoff erosion but does not capture mass wasting events related to landslides. This limitation in the model is a possible explanation for discrepancies between long-term VIC–WEPP estimates and observed. Finally, we were limited by a lack of fine-resolution sediment observations for model evaluation. Efforts are needed to increase the availability sediment observations for erosion and water quality studies, particularly given the likelihood of climate change and wildfire exacerbating current water quality problems.

6. Conclusions

We utilize a macro-scale hydrological model (VIC) and a high-resolution soil erosion model (WEPP-HE) to simulate grid cell level (~6 km × 6 km) sediment yield due to runoff erosion over a large and heterogeneous mountainous basin. Using this integrated framework (VIC–WEPP), we quantify the relative contributions of fire activity (for various fire severities) and climate change on streamflow and sediment yield.

The VIC–WEPP model results indicate that SRB streamflow will have an earlier spring peak flow by one to two months under future climate scenarios in response to a declining snowpack under warming temperatures. The magnitude of peak flow increases with each higher severity fire scenario; and under the highest fire severity, the peak flow is shifted even earlier, exacerbating the effects of climate change. Similarly, sediment yield also increases with higher fire severities for both historical and future climates. Sediment yield is more sensitive to fire occurrence than to climate change by one to two orders of magnitude, which is not unexpected given that our fire scenarios were applied basin wide as worst case scenarios. In reality, fires only occur over portions of the basin in any given year and subsequent years' vegetation regrowth reduces erosion. However, the effects of climate change on sediment yield result in greater spatial heterogeneities, primarily because of the spatial differences in precipitation projections, while fire conditions were uniformly applied. The combined effects of climate change and a possible continuation of increasing fire frequency and severity will compound excess sediment issues that already exist in this region of the intermountain West.

Acknowledgements

This research is funded by the Department of Agriculture, National Institute of Food and Agriculture Grant Number 2012-67003-19805 through the Water Sustainability and Climate program, and by the State of Washington Water Research Center Grant Number G11AP20113 through the United States Geological Survey 104(b) funding to the Water Resource Research Institutes. The authors would also like to thank Alan Hamlet for insights related to calibration of the VIC model over the Salmon River basin, Lili Wang for support in implementation of VIC–WEPP, and Joe Wagenbrenner for help in identifying parameters for WEPP in post-fire environments. Finally, we would like to thank two anonymous reviewers for their thoughtful comments that improved the manuscript.

ous reviewers for their thoughtful comments that improved the manuscript.

References

- Abatzoglou, J.T., 2013. Development of gridded surface meteorological data for ecological applications and modelling. *Int. J. Climatol.* 33, 121–131. <http://dx.doi.org/10.1002/joc.3413>.
- Abatzoglou, J.T., Brown, T.J., 2012. A comparison of statistical downscaling methods suited for wildfire applications. *Int. J. Climatol.* 32, 772–780. <http://dx.doi.org/10.1002/joc.2312>.
- Adam, J.C., Hamlet, A.F., Lettenmaier, D.P., 2009. Implications of global climate change for snowmelt hydrology in the twenty-first century. *Hydrol. Process.* 23, 962–972. <http://dx.doi.org/10.1002/hyp.7201>.
- Agee, J.K., 1993. *Fire Ecology of Pacific Northwest Forests*. Island Press.
- Andreadis, K.M., Storck, P., Lettenmaier, D.P., 2009. Modeling snow accumulation and ablation processes in forested environments. *Water Resour. Res.* 45. <http://dx.doi.org/10.1029/2008WR007042>.
- Arnold, J., Srinivasan, R., Mutiah, R., Williams, J., 1998. Large area hydrologic modeling and assessment – Part 1: Model development. *J. Am. Water Resour. Assoc.* 34, 73–89. <http://dx.doi.org/10.1111/j.1752-1688.1998.tb05961.x>.
- Barsugli, J.J., Elsner, M.M., Hamlet, A.F., 2012. Building a Stronger and More Extensive Hydrologic Foundation for Environmental Flow and Climate Change Research across the Colorado River Basin (Final Report Prepared for The Nature Conservancy).
- Benavides-Solorio, J., MacDonald, L., 2005. Measurement and prediction of post-fire erosion at the hillslope scale, Colorado Front Range. *Int. J. Wildland Fire* 14, 457–474. <http://dx.doi.org/10.1071/WF05042>.
- Benavides-Solorio, J., MacDonald, L., 2001. Post-fire runoff and erosion from simulated rainfall on small plots, Colorado Front Range. *Hydrol. Process.* 15, 2931–2952. <http://dx.doi.org/10.1002/hyp.383>.
- Bohn, T.J., Livneh, B., Oyler, J.W., Running, S.W., Nijssen, B., Lettenmaier, D.P., 2013. Global evaluation of MTCLIM and related algorithms for forcing of ecological and hydrological models. *Agri. Forest. Meteorol.* 38–49. <http://dx.doi.org/10.1016/j.agrformet.2013.03.003>.
- Boll, J., Brooks, E., McAtty, J., Barber, M., Ullman, J., McCool, D., Lu, X., Lawler, A., Ryan, J., 2011. Evaluation of Sediment Yield Reduction Potential in Agricultural and Mixed-use Watersheds of the Lower Snake River basin (Technical Report, Submitted to US Army Corps of Engineers by State of Washington Water Research Center, Pullman, WA).
- Bowling, L.C., Lettenmaier, D.P., 2010. Modeling the effects of lakes and wetlands on the water balance of arctic environments. *J. Hydrometeorol.* 11, 276–295. <http://dx.doi.org/10.1175/2009JHM1084.1>.
- Bowling, L.C., Pomeroy, J.W., Lettenmaier, D.P., 2004. Parameterization of blowing-snow sublimation in a macroscale hydrology model. *J. Hydrometeorol.* 5, 745–762. [http://dx.doi.org/10.1175/1525-7541\(2004\)005<0745:POBSIA>2.0.CO;2](http://dx.doi.org/10.1175/1525-7541(2004)005<0745:POBSIA>2.0.CO;2).
- Cherkauer, K., Lettenmaier, D., 1999. Hydrologic effects of frozen soils in the upper Mississippi River basin. *J. Geophys. Res. Atmos.* 104, 19599–19610. <http://dx.doi.org/10.1029/1999JD900337>.
- Chuvieco, E., Martinez, S., Victoria Roman, M., Hantson, S., Lucrecia Pettinari, M., 2014. Integration of ecological and socio-economic factors to assess global vulnerability to wildfire. *Glob. Ecol. Biogeogr.* 23, 245–258. <http://dx.doi.org/10.1111/geb.12095>.
- Connaughton, C.A., 1935. Forest fires and accelerated erosion. *intermountain forest and range experiment station. J. For.* 33, 751–752.
- Coulibaly, P., Bobee, B., Anctil, F., 2001. Improving extreme hydrologic events forecasting using a new criterion for artificial neural network selection. *Hydrol. Process.* 15, 1533–1536. <http://dx.doi.org/10.1002/hyp.445>.
- Cui, X., Gao, F., Song, J., Sang, Y., Sun, J., Di, X., 2014. Changes in soil total organic carbon after an experimental fire in a cold temperate coniferous forest: a sequenced monitoring approach. *Geoderma* 226, 260–269. <http://dx.doi.org/10.1016/j.geoderma.2014.02.010>.
- Dai, A., 2011. Drought under global warming: a review. *Wiley Interdiscip. Rev. Clim. Change* 2, 45–65. <http://dx.doi.org/10.1002/wcc.81>.
- Daly, C., Halbleib, M., Smith, J.L., Gibson, W.P., Doggett, M.K., Taylor, G.H., Curtis, J., Pasteris, P.P., 2008. Physiographically sensitive mapping of climatological temperature and precipitation across the conterminous United States. *Int. J. Climatol.* 28, 2031–2064. <http://dx.doi.org/10.1002/joc.1688>.
- Danielson, J.J., Gesch, D.B., 2011. Global Multi-resolution Terrain Elevation Data 2010 (GMTED2010) (No. 2011-1073). Open-File Report. U.S. Geological Survey.
- DeBano, L.F., Neary, D.J., Ffolliott, P.F., 2005. Soil physical properties (General Technical Report No. RMRS-GTR-42). In: Neary, D.G., Ryan, K.C., DeBano, L.F. (Eds.), *Wildland Fire in Ecosystems: Effects of Fire on Soils and Water*. U.S. Department of Agriculture, Forest Service, Rocky Mountain Research Station, Ogden, UT.
- Doerr, S.H., Shakesby, R.A., Blake, W.H., Chafer, C.J., Humphreys, G.S., Wallbrink, P.J., 2006. Effects of differing wildfire severities on soil wettability and implications for hydrological response. *J. Hydrol.* 319, 295–311. <http://dx.doi.org/10.1016/j.jhydrol.2005.06.038>.
- Ebel, B.A., Moody, J.A., 2013. Rethinking infiltration in wildfire-affected soils. *Hydrol. Process.* 27, 1510–1514. <http://dx.doi.org/10.1002/hyp.9696>.
- Ebel, B.A., Moody, J.A., Martin, D.A., 2012. Hydrologic conditions controlling runoff generation immediately after wildfire. *Water Resour. Res.* 48, W03529. <http://dx.doi.org/10.1029/2011WR011470>.

- Elliot, W.J., 2013. Erosion processes and prediction with WEPP technology in forests in the northwestern U.S. *Trans. ASABE* 56, 563–579.
- Elliot, W.J., Hall, D.E., 2010. Disturbed WEPP Model 2.0. Ver. 2011.11.22. U.S. Department of Agriculture, Forest Service, Rocky Mountain Research Station, Moscow, ID.
- Elsner, M.M., Cuo, L., Voisin, N., Deems, J.S., Hamlet, A.F., Vano, J.A., Mickelson, K.E.B., Lee, S.-Y., Lettenmaier, D.P., 2010. Implications of 21st century climate change for the hydrology of Washington State. *Clim. Change* 102, 225–260. <http://dx.doi.org/10.1007/s10584-010-9855-0>.
- Espinosa, F.A., Rhodes, J.J., McCullough, D.A., 1997. The failure of existing plans to protect salmon habitat in the Clearwater National Forest in Idaho. *J. Environ. Manage.* 49, 205–230.
- Flanagan, D.C., Ascough, J.C., Geter, W.F., David, O., 2005. Development of a hillslope erosion module for the object modeling system. Presented at the ASAE Annual International Meeting, ASAE, St. Joseph, MI, Tampa, FL, USA.
- Flanagan, D.C., Nearing, M.A., 1995. USDA – Water Erosion Prediction Project: Hillslope Profile and Watershed Model Documentation. West Lafayette, IN.
- Foster, G., Yoder, D.C., McCool, D., Weesies, G., Toy, T.J., Wagner, L.E., 2000. Improvements in Science in RUSLE2 (No. Paper No. 00-2147). ASAE, 2950 Niles Rd., St. Joseph, MI 439085-9659, USA.
- Frankenberger, J.R., Dun, S., Flanagan, D.C., Wu, J.Q., Elliot, W.J., 2011. Development of a GIS Interface for WEPP Model Application to Great Lakes Forested Watersheds. Presented at the International Symposium on Erosion and Landscape Evolution, ISELE, Anchorage, Alaska.
- Friedli, M., McIver, D., Hodges, J., Zhang, X., Muchoney, D., Strahler, A., Woodcock, C., Gopal, S., Schneider, A., Cooper, A., Baccini, A., Gao, F., Schaaf, C., 2002. Global land cover mapping from MODIS: algorithms and early results. *Remote Sens. Environ.* 83, 287–302. [http://dx.doi.org/10.1016/S0034-4257\(02\)00078-0](http://dx.doi.org/10.1016/S0034-4257(02)00078-0).
- Gao, H., Tang, Q., Shi, X., Zhu, C., Bohn, T., Su, F., Sheffield, J., Pan, M., Lettenmaier, D.P., Wood, E.F., 2010. Water budget record from Variable Infiltration Capacity (VIC) Model. In: Algorithm Theoretical Basis Document for Terrestrial Water Cycle Data Records.
- Goode, J.R., Luce, C.H., Buffington, J.M., 2012. Enhanced sediment delivery in a changing climate in semi-arid mountain basins: implications for water resource management and aquatic habitat in the northern Rocky Mountains. *Geomorphology* 139, 1–15. <http://dx.doi.org/10.1016/j.geomorph.2011.06.021>.
- Hamlet, A.F., Elsner, M.M., Mauder, G., Lee, S.-Y., Tohver, I., Norheim, R.A., 2013. An overview of the Columbia Basin climate change scenarios project: approach, methods, and summary of key results. *Atmos. Ocean* 392–415. <http://dx.doi.org/10.1080/07055900.2013.819555>.
- Hamlet, A., Lettenmaier, D., 1999. Effects of climate change on hydrology and water resources in the Columbia River basin. *J. Am. Water Resour. Assoc.* 35, 1597–1623. <http://dx.doi.org/10.1111/j.1752-1688.1999.tb04240.x>.
- Helvey, J.D., 1980. Effects of a north central Washington wildfire on runoff and sediment production. *Water Resour. Bull.* 16, 627–634.
- Hill, R.D., Peart, M.R., 1998. Land use, runoff, erosion and their control: a review for southern China. *Hydrol. Process.* 12, 2029–2042. [http://dx.doi.org/10.1002/\(SICI\)1099-1085\(19981030\)12:13<14<2029::AID-HYP717>3.0.CO;2-O](http://dx.doi.org/10.1002/(SICI)1099-1085(19981030)12:13<14<2029::AID-HYP717>3.0.CO;2-O).
- Holden, Z.A., Luce, C.H., Crimmins, M.A., Morgan, P., 2012. Wildfire extent and severity correlated with annual streamflow distribution and timing in the Pacific Northwest, USA (1984–2005). *Ecohydrology* 5, 677–684. <http://dx.doi.org/10.1002/eco.257>.
- Hungerford, R., Nemani, R., Running, S.W., Coughlan, J.C., 1989. MTCLIM – A Mountain Microclimate Simulation-model. USDA For. Serv. Intermt. Res. Stn. Res. Pap. 1–52.
- Johansen, M., Hakonson, T., Breshears, D., 2001. Post-fire runoff and erosion from rainfall simulation: contrasting forests with shrublands and grasslands. *Hydrol. Process.* 15, 2953–2965. <http://dx.doi.org/10.1002/hyp.384>.
- Jolly, W.M., Cochrane, M.A., Freeborn, P.H., Holden, Z.A., Brown, T.J., Williamson, G.J., Bowman, D.M.J.S., 2015. Climate-induced variations in global wildfire danger from 1979 to 2013. *Nat Commun* 6.
- Karamesouti, M., Petropoulos, G.P., Papanikolaou, I.D., Kairis, O., Kosmas, K., 2016. Erosion rate predictions from PESERA and RUSLE at a Mediterranean site before and after a wildfire: comparison & implications. *Geoderma* 261, 44–58. <http://dx.doi.org/10.1016/j.geoderma.2015.06.025>.
- Karl, T.R., Meehl, G.A., Miller, C.D., Hassol, S.J., Waple, A.M., Murray, W.L. (Eds.), 2008. Weather and climate extremes in a changing climate. Regions of Focus: North America, Hawaii, Caribbean, and U.S. Pacific Islands. Department of Commerce, NOAA's National Climatic Data Center, Washington, D.C.
- Kimball, J., Running, S., Nemani, R., 1997. An improved method for estimating surface humidity from daily minimum temperature. *Agric. For. Meteorol.* 85, 87–98. [http://dx.doi.org/10.1016/S0168-1923\(96\)02366-0](http://dx.doi.org/10.1016/S0168-1923(96)02366-0).
- Kirchner, J.W., Finkel, R.C., Riebe, C.S., Granger, D.E., Clayton, J.L., King, J.G., Megahan, W.F., 2001. Mountain erosion over 10 yr, 10 k.y., and 10 m.y. time scales. *Geology* 29, 591–594. [http://dx.doi.org/10.1130/0091-7613\(2001\)029<0591:MEQYK>2.0.CO;2](http://dx.doi.org/10.1130/0091-7613(2001)029<0591:MEQYK>2.0.CO;2).
- Kirschbaum, R.L., Lettenmaier, D.P., 1997. An Evaluation of the Effects of Anthropogenic Activity on Streamflow in the Columbia River Basin (No. 156). Water Resources Series Tech. Rep. University of Washington, Department of Civil Engineering, Seattle, WA, USA.
- Klinkenberg, B., Goodchild, M., 1992. The fractal properties of topography – a comparison of methods. *Earth Surf. Process. Landf.* 17, 217–234. <http://dx.doi.org/10.1002/esp.3290170303>.
- Lafren, J., Elliot, W.J., Simanton, J., Holzhey, C., Kohl, K., 1991. WEPP – soil erodibility experiments for rangeland and cropland soils. *J. Soil Water Conserv.* 46, 39–44.
- Langhans, C., Smith, H.G., Chong, D.M.O., Nyman, P., Lane, P.N.J., Sheridan, G.J., 2016. A model for assessing water quality risk in catchments prone to wildfire. *J. Hydrol.* 534, 407–426.
- Larsen, I.J., MacDonald, L.H., Brown, E., Rough, D., Welsh, M.J., Pietraszek, J.H., Libohova, Z., de Dios Benavides-Solorio, J., Schaffrath, K., 2009. Causes of post-fire runoff and erosion: water repellency, cover, or soil sealing? *Soil Sci. Soc. Am. J.* 73, 1393–1407. <http://dx.doi.org/10.2136/sssaj2007.0432>.
- Leonard, R., Knisel, W., Still, D., 1987. GLEAMS – groundwater loading effects of agricultural management-systems. *Trans. ASABE* 30, 1403–1418.
- Leung, L., Qian, Y., Bian, X., Washington, W., Han, J., Roads, J., 2004. Mid-century ensemble regional climate change scenarios for the western United States. *Clim. Change* 62, 75–113. <http://dx.doi.org/10.1023/B:CLIM.0000013692.50640.55>.
- Liang, X., Lettenmaier, D.P., Wood, E.F., Burges, S.J., 1994. A simple hydrologically based model of land-surface water and energy fluxes for general-circulation models. *J. Geophys. Res. Atmos.* 99, 14415–14428. <http://dx.doi.org/10.1029/94JD00483>.
- Liu, M., Adam, J.C., Hamlet, A.F., 2013. Spatial-temporal variations of evapotranspiration and runoff/precipitation ratios responding to the changing climate in the Pacific Northwest during 1921–2006. *J. Geophys. Res.* 118, 380–394. <http://dx.doi.org/10.1029/2012JD018400>.
- Liu, M., Rajagopalan, K., Chung, S.H., Jiang, X., Harrison, J., Nergui, T., Guenther, A., Miller, C., Reyes, J., Tague, C., Choate, J., Salathe, E.P., Stoeckle, C.O., Adam, J.C., 2014. What is the importance of climate model bias when projecting the impacts of climate change on land surface processes? *Biogeosciences* 11, 2601–2622. <http://dx.doi.org/10.5194/bg-11-2601-2014>.
- Lohmann, D., Nolte-Holube, R., Raschke, E., 1996. A large-scale horizontal routing model to be coupled to land surface parametrization schemes. *Tellus Ser. Dyn. Meteorol. Oceanogr.* 48, 708–721. <http://dx.doi.org/10.1034/j.1600-0870.1996.t01-3-00009.x>.
- Lohmann, D., Raschke, E., Nijssen, B., Lettenmaier, D.P., 1998. Regional scale hydrology: I. Formulation of the VIC-2L model coupled to a routing model. *Hydrol. Sci. J.* 43, 131–141. <http://dx.doi.org/10.1080/02626669809492107>.
- Lown, J.B., Lyon, J.P., Yoder, D.C., 2000. A Scientific Modeling Architecture to Simultaneously Meet Needs of Scientists, Programmers, Data Managers, and End-Users (No. Paper No. 003051). ASAE, 2950 Niles Rd., St. Joseph, MI 439085-9659, USA.
- Mahat, V., Anderson, A., Silins, U., 2015. Modelling of wildfire impacts on catchment hydrology applied to two case studies. *Hydrol. Process.* 29, 3687–3698. <http://dx.doi.org/10.1002/hyp.10462>.
- Mao, D., Cherkauer, K.A., Flanagan, D.C., 2010. Development of a coupled soil erosion and large-scale hydrology modeling system. *Water Resour. Res.* 46, W08543. <http://dx.doi.org/10.1029/2009WR008268>.
- Maurer, E.P., Wood, A.W., Adam, J.C., Lettenmaier, D.P., Nijssen, B., 2002. A long-term hydrologically based dataset of land surface fluxes and states for the conterminous United States. *J. Clim.* 15, 3237–3251. [http://dx.doi.org/10.1175/1520-0442\(2002\)015<3237:ALHTBD>2.0.CO;2](http://dx.doi.org/10.1175/1520-0442(2002)015<3237:ALHTBD>2.0.CO;2).
- Miles, E., Snover, A., Hamlet, A., Callahan, B., Fluharty, D., 2000. Pacific northwest regional assessment: the impacts of climate variability and climate change on the water resources of the Columbia River Basin. *J. Am. Water Resour. Assoc.* 36, 399–420. <http://dx.doi.org/10.1111/j.1752-1688.2000.tb04277.x>.
- Mitchell, K.E., Lohmann, D., Houser, P.R., Wood, E.F., Schaake, J.C., Robock, A., Cosgrove, B.A., Sheffield, J., Duan, Q., Luo, L., Higgins, R.W., Pinker, R.T., Tarpley, J. D., Lettenmaier, D.P., Marshall, C.H., Entin, J.K., Pan, M., Shi, W., Koren, V., Meng, J., Ramsay, B.H., Bailey, A.A., 2004. The multi-institution North American Land Data Assimilation System (NLDAS): utilizing multiple GCM products and partners in a continental distributed hydrological modeling system. *J. Geophys. Res. Atmos.* 109. <http://dx.doi.org/10.1029/2003JD003823>.
- Moody, J.A., Martin, D.A., 2014. Fostering post-wildfire research. *Eos Trans. AGU* 95, 37.
- Moody, J.A., Martin, D.A., 2009. Synthesis of sediment yields after wildland fire in different rainfall regimes in the western United States. *Int. J. Wildland Fire* 18, 96–115. <http://dx.doi.org/10.1071/WF07162>.
- Moody, J.A., Martin, D.A., 2001a. Initial hydrologic and geomorphic response following a wildfire in the Colorado Front Range. *Earth Surf. Process. Landf.* 26, 1049–1070. <http://dx.doi.org/10.1002/esp.253>.
- Moody, J.A., Martin, D.A., 2001b. Post-fire, rainfall intensity-peak discharge relations for three mountainous watersheds in the western USA. *Hydrol. Process.* 15, 2981–2993. <http://dx.doi.org/10.1002/hyp.386>.
- Moody, J.A., Martin, D.A., Cannon, S.H., 2008. Post-wildfire erosion response in two geologic terrains in the western USA. *Geomorphology* 95, 103–118. <http://dx.doi.org/10.1016/j.geomorph.2007.05.011>.
- Moody, J.A., Shakesby, R.A., Robichaud, P.R., Cannon, S.H., Martin, D.A., 2013. Current research issues related to post-wildfire runoff and erosion processes. *Earth-Sci. Res.* 122, 10–37. <http://dx.doi.org/10.1016/j.earscirev.2013.03.004>.
- Moriassi, D.N., Arnold, J.G., Van Liew, M.W., Bingner, R.L., Harmel, R.D., Veith, T.L., 2007. Model evaluation guidelines for systematic quantification of accuracy in watershed simulations. *Trans. ASABE* 50, 885–900.
- Mote, P., Hamlet, A., Clark, M., Lettenmaier, D., 2005. Declining mountain snowpack in western North America. *Bull. Am. Meteorol. Soc.* 86, 39–49. <http://dx.doi.org/10.1175/BAMS-86-1-39>.
- Mote, P.W., Salathe Jr., E.P., 2010. Future climate in the Pacific Northwest. *Clim. Change* 102, 29–50. <http://dx.doi.org/10.1007/s10584-010-9848-z>.
- Nijssen, B., Lettenmaier, D., Liang, X., Wetzel, S., Wood, E., 1997. Streamflow simulation for continental-scale river basins. *Water Resour. Res.* 33, 711–724. <http://dx.doi.org/10.1029/96WR03517>.

- Nyman, P., Sheridan, G.J., Lane, P.N.J., 2013. Hydro-geomorphic response models for burned areas and their applications in land management. *Prog. Phys. Geogr.* 37, 787–812. <http://dx.doi.org/10.1177/0309133313508802>.
- Nyman, P., Smith, H.G., Sherwin, C.B., Langhans, C., Lane, P.N.J., Sheridan, G.J., 2015. Predicting sediment delivery from debris flows after wildfire. *Geomorphology* 250, 173–186. <http://dx.doi.org/10.1016/j.geomorph.2015.08.023>.
- Owens, P.N., Batalla, R.J., Collins, A.J., Gomez, B., Hicks, D.M., Horowitz, A.J., Kondolf, G.M., Marden, M., Page, M.J., Peacock, D.H., Petticrew, E.L., Salomons, W., Trustrum, N.A., 2005. Fine-grained sediment in river systems: environmental significance and management issues. *River Res. Appl.* 21, 693–717. <http://dx.doi.org/10.1002/rra.878>.
- Park, S.J., van de Giesen, N., 2004. Soil-landscape delineation to define spatial sampling domains for hillslope hydrology. *J. Hydrol.* 295, 28–46. <http://dx.doi.org/10.1016/j.jhydrol.2004.02.022>.
- Parson, A., Robichaud, P.R., Lewis, S.A., Napper, C., Clark, J.T., 2010. Field Guide for Mapping Post-fire Soil Burn Severity (Gen. Tech. Rep. No. RMRS-GTR-243). Department of Agriculture, Forest Service, Rocky Mountain Research Station, Fort Collins, CO., USA.
- Randerson, J.T., van der Werf, G.R., Giglio, L., Collatz, G.J., Kasibhatla, P.S., 2015. Global Fire Emissions Database, Version 4, (GFEDv4).
- Renard, K., Foster, G., Weesies, G., Porter, J., 1991. RUSLE – revised universal soil loss equation. *J. Soil Water Conserv.* 46, 30–33.
- Reneau, S.L., Katzman, D., Kuyumjian, G.A., Lavine, A., Malmon, D.V., 2007. Sediment delivery after a wildfire. *Geology* 35, 151–154. <http://dx.doi.org/10.1130/G23288A.1>.
- Robertson, M.J., Scruton, D.A., Clarke, K.D., 2007. Seasonal effects of suspended sediment on the behavior of juvenile Atlantic salmon. *Trans. Am. Fish. Soc.* 136, 822–828. <http://dx.doi.org/10.1577/T06-164.1>.
- Robichaud, P.R., 2000. Fire effects on infiltration rates after prescribed fire in Northern Rocky Mountain forests, USA. *J. Hydrol.* 231, 220–229. [http://dx.doi.org/10.1016/S0022-1694\(00\)00196-7](http://dx.doi.org/10.1016/S0022-1694(00)00196-7).
- Robichaud, P.R., Elliot, W.J., Pierson, F.B., Hall, D.E., Moffet, C.A., 2007. Predicting postfire erosion and mitigation effectiveness with a web-based probabilistic erosion model. *Catena* 71, 229–241. <http://dx.doi.org/10.1016/j.catena.2007.03.003>.
- Robichaud, P.R., Wagenbrenner, J.W., Brown, R.E., 2010. Rill erosion in natural and disturbed forests: 1. Measurements. *Water Resour. Res.* 46, W10506. <http://dx.doi.org/10.1029/2009WR008314>.
- Shin, S.S., Park, S.D., Lee, K.S., 2013. Sediment and hydrological response to vegetation recovery following wildfire on hillslopes and the hollow of a small watershed. *J. Hydrol.* 499, 154–166. <http://dx.doi.org/10.1016/j.jhydrol.2013.06.048>.
- Silins, U., Bladon, K.D., Kelly, E.N., Esch, E., Spence, J.R., Stone, M., Emelko, M.B., Boon, S., Wagner, M.J., Williams, C.H.S., Tichkowsky, I., 2014. Five-year legacy of wildfire and salvage logging impacts on nutrient runoff and aquatic plant, invertebrate, and fish productivity. *Ecohydrology* 7, 1508–1523. <http://dx.doi.org/10.1002/eco.1474>.
- Silins, U., Stone, M., Emelko, M.B., Bladon, K.D., 2009. Sediment production following severe wildfire and post-fire salvage logging in the Rocky Mountain headwaters of the Oldman River Basin, Alberta. *Catena* 79, 189–197. <http://dx.doi.org/10.1016/j.catena.2009.04.001>.
- Silins, U., Stone, M., Emelko, M.B., Bladon, K.D., 2008. Impacts of wildfire and post-fire salvage logging on sediment transfer in the Oldman watershed, Alberta, Canada. In: *Sediment Dynamics in Changing Environments*. IAHS Publ., Christchurch, New Zealand.
- Sridhar, V., Jin, X., Jaks, W.T.A., 2013. Explaining the hydroclimatic variability and change in the Salmon River basin. *Clim. Dyn.* 40, 1921–1937. <http://dx.doi.org/10.1007/s00382-012-1467-0>.
- Stephens, S., Ruth, L., 2005. Federal forest-fire policy in the United States. *Ecol. Appl.* 15, 532–542. <http://dx.doi.org/10.1890/04-0545>.
- Tang, C., Crosby, B.T., Wheaton, J.M., Piechota, T.C., 2012. Assessing streamflow sensitivity to temperature increases in the Salmon River Basin, Idaho. *Glob. Planet. Change* 88–89, 32–44. <http://dx.doi.org/10.1016/j.gloplacha.2012.03.002>.
- Tang, Q., Lettenmaier, D.P., 2012. 21st century runoff sensitivities of major global river basins. *Geophys. Res. Lett.* 39. <http://dx.doi.org/10.1029/2011GL050834>.
- Teasdale, G.N., Barber, M.E., 2008. Aerial assessment of ephemeral gully erosion from agricultural regions in the Pacific Northwest. *J. Irrig. Drain. Eng. ASCE* 134, 807–814. [http://dx.doi.org/10.1061/\(ASCE\)0733-9437\(2008\)134:6\(807\)](http://dx.doi.org/10.1061/(ASCE)0733-9437(2008)134:6(807)).
- Tetra Tech EC, Inc., 2006. Investigation of Sediment Source and Yield, Management, and Restoration Opportunities within the Lower Snake River Basin (Contract W912EF-05-D-002). U.S. Army Corps of Engineers, Walla Walla District.
- Thompson, J.A., Pena-Yewtukhiw, E.M., Grove, J.H., 2006. Soil-landscape modeling across a physiographic region: topographic patterns and model transportability. *Geoderma* 133, 57–70. <http://dx.doi.org/10.1016/j.geoderma.2006.03.037>.
- Thornton, P., Hasenauer, H., White, M., 2000. Simultaneous estimation of daily solar radiation and humidity from observed temperature and precipitation: an application over complex terrain in Austria. *Agric. For. Meteorol.* 104, 255–271. [http://dx.doi.org/10.1016/S0168-1923\(98\)00170-2](http://dx.doi.org/10.1016/S0168-1923(98)00170-2).
- Thornton, P., Running, S., 1999. An improved algorithm for estimating incident daily solar radiation from measurements of temperature, humidity, and precipitation. *Agric. For. Meteorol.* 93, 211–228. [http://dx.doi.org/10.1016/S0168-1923\(98\)00126-9](http://dx.doi.org/10.1016/S0168-1923(98)00126-9).
- United States Department of Agriculture, 1994. State Soil Geographic (STATSGO) Data Base: Data Use Information, Miscellaneous (No. Publication No. 1492 (revised edition)). US Department of Agriculture, National Resources Conservation Service, Forth Worth, Texas, USA.
- U.S. Army Corps of Engineers, 2012. Lower Snake River Programmatic Sediment Management Plan/Environmental Impact Statement (Draft). U.S. Army Corps of Engineers Walla Walla District.
- US Global Change Research Program, 2012. The National Global Change Research Plan 2012–2021: A Strategic Plan for the US Global Change Research Program. Washington, DC.
- Wagenbrenner, J.W., Robichaud, P.R., Elliot, W.J., 2010. Rill erosion in natural and disturbed forests: 2. Modeling approaches. *Water Resour. Res.* 46, W10507. <http://dx.doi.org/10.1029/2009WR008315>.
- Westerling, A.L., Hidalgo, H.G., Cayan, D.R., Swetnam, T.W., 2006. Warming and earlier spring increase western US forest wildfire activity. *Science* 313, 940–943. <http://dx.doi.org/10.1126/science.1128834>.
- Williams, J., Nicks, A., Arnold, J., 1985. Simulator for water-resources in rural basins. *J. Hydraul. Eng. ASCE* 111, 970–986.
- Williams, J.R., Berndt, H.D., 1977. Sediment yield prediction based on watershed hydrology. *Trans. Am. Soc. Agric. Eng.* 20, 1100–1104.
- Wischmeier, W.H., Smith, D.D., 1978. Predicting Rainfall Erosion Losses – A Guide to Conservation Planning, Agriculture Handbook. US Department of Agriculture, Washington, DC.
- Wood, P.J., Armitage, P.D., 1997. Biological effects of fine sediment in the lotic environment. *Environ. Manage.* 21, 203–217. <http://dx.doi.org/10.1007/s002679900019>.
- Xu, T., Moore, I., Gallant, J., 1993. Fractals, fractal dimensions and landscapes – a review. *Geomorphology* 8, 245–262. [http://dx.doi.org/10.1016/0169-555X\(93\)90022-T](http://dx.doi.org/10.1016/0169-555X(93)90022-T).
- Zhang, X.Y., Drake, N.A., Wainwright, J., Mulligan, M., 1999. Comparison of slope estimates from low resolution DEMs: scaling issues and a fractal method for their solution. *Earth Surf. Process. Landf.* 24, 763–779. [http://dx.doi.org/10.1002/\(SICI\)1096-9837\(199908\)24:9<763::AID-ESP9>3.0.CO;2-J](http://dx.doi.org/10.1002/(SICI)1096-9837(199908)24:9<763::AID-ESP9>3.0.CO;2-J).